

Causal Structural Learning Via Local Graphs*

Wenyu Chen¹, Mathias Drton², and Ali Shojaie³

¹Department of Statistics, University of Washington, Seattle, WA, USA

²Department of Mathematics, Technical University of Munich, München, Germany

³Department of Biostatistics, University of Washington, Seattle, WA, USA

January 2, 2022

Abstract

We consider the problem of learning causal structures in sparse high-dimensional settings that may be subject to the presence of (potentially many) unmeasured confounders, as well as selection bias. Based on the structure found in common families of large random networks and examining the representation of local structures in linear structural equation models (SEM), we propose a new local notion of sparsity for consistent structure learning in the presence of latent and selection variables, and develop a new version of the Fast Causal Inference (FCI) algorithm with reduced computational and sample complexity, which we refer to as local FCI (lFCI). The new notion of sparsity allows the presence of highly connected hub nodes, which are common in real-world networks, but problematic for existing methods. Our numerical experiments indicate that the lFCI algorithm achieves state-of-the-art performance across many classes of large random networks, and its performance is superior to that of existing methods for networks containing hub nodes.

1 Introduction

Directed graphical models are commonly used to model causal relations between random variables in complex systems (Maathuis et al., 2019). In this framework, each random variable is a function of other variables (its causes) and stochastic noise. The causal relations are represented by a directed acyclic graph (DAG), with vertices representing random variables, and directed edges representing direct causal effects. While different DAGs may yield the same model for observational data, their Markov equivalence class can be represented by a unique completed partially directed acyclic graph (CPDAG). When all relevant variables are observed, a variety of techniques exist for learning the CPDAG from observational data; one of the most commonly used is the PC algorithm (Spirtes et al., 2000), which is also the basis for many other constraint-based and hybrid algorithms (see, e.g., Tsamardinos et al., 2006; Ogarrio et al., 2016). The PC algorithm is sound and complete (Spirtes et al., 2000), and consistent in sparse high-dimensional settings (Kalisch and Bühlmann, 2007).

Observational studies often involve latent variables (i.e., variables that remain unmeasured) as well as selection variables conditional on which the observations are made. Ignoring latent and selection variables may invalidate causal conclusions. To account for their presence, the ancestral relationships and conditional independences among the observed variables can be represented by a maximal ancestral graph (MAG). As multiple MAGs may represent the same conditional independences, the target of estimation is the Markov equivalence class of these MAGs, which can be represented by a partial ancestral graph (PAG) (Ali et al., 2009).

PAGs can be learned from data on the observed variables using the FCI algorithm (Spirtes et al., 2000). The FCI algorithm uses the fact that two nodes i and j are non-adjacent in the PAG if and only if the corresponding variables are conditionally independent given their D-SEP set (d -separation set). This D-SEP set is comprised of ancestors that are adjacent or connected via certain collider paths (Spirtes et al., 2000). Since the D-SEP sets cannot be inferred directly, the FCI algorithm does not directly estimate the skeleton (i.e., adjacencies) of the PAG. Instead, FCI first uses an initial phase of the PC algorithm to obtain a preliminary skeleton, which is a superset of the PAG skeleton. It then uses the

*This work was supported by funding from the U.S. National Science Foundation (NSF) under grant DMS-1561814, U.S. National Institutes of Health (NIH) under grant R01GM114029, and the European Research Council (ERC) under the European Union's Horizon 2020 research and innovation programme (grant agreement No 883818).

PC output to compute supersets of the D-SEP sets, referred to as p-D-SEP sets (possible-D-SEP sets), and estimates the final skeleton using the p-D-SEP sets. To infer the skeleton, PC and the second step of FCI both adopt a hierarchical search strategy, wherein edges are removed recursively via tests of conditional independence given subsets of increasingly larger sizes in some search pool (neighbors in PC, p-D-SEP sets in FCI); see Section 4.1 for more details.

The FCI algorithm is consistent and complete in high-dimensional settings (Zhang, 2008; Colombo et al., 2012), but it is computationally expensive. This is partly because the p-D-SEP sets can be very large, leaving the final skeleton estimation step too many subsets to search amongst. Colombo et al. (2012) introduced multiple approaches for narrowing down the p-D-SEP sets, for example, by intersecting the sets with a bi-connected component (FCI_{path}), or applying conservative ordering rules (CFCI). They also proposed a fast approximation to the FCI algorithm, called RFCI, which directly estimates the final skeleton along with modified orientations, hence avoiding the computation of the p-D-SEP sets. The RFCI output, in which the presence of an edge between two nodes only implies conditional dependence given subsets of their neighborhood, is generally less informative than a PAG. To reduce the cost of estimating the initial skeleton, an anytime version of FCI was proposed in Spirtes (2001), and can be combined with the above modifications, but the skeleton it learns is only guaranteed to be a superset of the skeleton learned using FCI, and is therefore less informative. Claassen et al. (2013) proposed FCI+, based on an alternative construction of p-D-SEP sets. For networks with bounded maximal node degree, FCI+ has polynomial complexity in the number of nodes.

The outlined existing versions of the FCI algorithm all follow a *neighborhood-based search strategy*, in the sense that they search for separating sets among neighbors (in the PC step) and extended neighbors (in the p-D-SEP step). The computational and sample complexity of such neighborhood-based methods (including also the PC algorithm) scales with the size of the largest separator, which often scales with the maximum node degree of the graph; this is problematic in the presence of highly connected *hub nodes*, i.e., nodes with large degrees. Hub nodes abound in many real-world systems, such as biological networks and the Web (Chen and Sharp, 2004; Kleinberg et al., 1999). These networks are well-approximated by the family of power-law graphs, which have unbounded maximum degree (Kleinberg et al., 1999).

Instead of relying on the common sparsity assumption via bounded maximum node degree, in this paper we exploit a *local-separation property* that holds for many large random networks. While this property — which also holds for power-law graphs containing hub nodes (Malioutov et al., 2006) — does not restrict the total number of paths between every pair of nodes, it implies a small number of *short paths* between them. The notion is illustrated in Figure 1 and is formalized in Section 3. The property motivates us to switch the focus from D-SEP sets to *local* D-SEP sets — that is, separators with respect to short paths. Accordingly, we shift from the neighborhood-based search strategy to a *local-graph-based search strategy*. Under the local-separation property, together with an alternative set of assumptions discussed in Section 5, this strategy enjoys reduced computational and sample complexity.

Concretely, in this work, we propose a new *local FCI* (lFCI) algorithm for structure learning in the presence of latent and selection variables. The lFCI algorithm learns the skeleton of a PAG by testing conditional independences between pairs of nodes (i, j) given sets of small cardinality. However, in contrast to other algorithms, the conditioning sets are selected only from the nodes that are within short distance (therefore, local) to $\{i, j\}$. By doing so, under a different set of assumptions than those considered for FCI, lFCI can learn networks with p nodes and $O(p^a)$ maximal node degree ($a > 1$) in polynomial computational and sample complexity — in such cases, the complexity of FCI is exponential in p .

A similar idea has recently been employed in the *reduced PC* (rPC) algorithm (Sondhi and Shojaie, 2019). In the setting without latent or selection variables, rPC may offer reduced computational and sample complexity compared to PC. However, latent and selection variables as considered here pose new challenges that cannot be addressed by simply replacing the PC steps in FCI with rPC steps. This is because rPC uses a notion of local separation in undirected graphs that does not naturally extend to mixed graphs. In addition, while rPC justifies focus on small conditioning sets through a local perspective, it does not follow the local-graph-based strategy adopted in our new lFCI. As a result, for any pair of nodes, rPC searches for separating sets among all other $p - 2$ nodes, which can be computationally prohibitive. Beyond a reduction in computational cost, our local-graph-based strategy leads to high-dimensional consistency under less restrictive assumptions than those in Sondhi and Shojaie (2019).

The paper begins with some preliminaries in Section 2, after which we introduce graph-theoretic results on local separation in Section 3. The lFCI algorithm is presented in Section 4 and its consistency for linear SEM is established in Section 5. We illustrate the

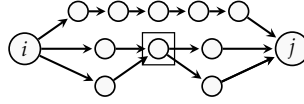


Figure 1: Illustration of a γ -local separator between i and j (shown in box) with $\gamma = 4$. There are 4 short paths between i and j , and the local separator is not a d-separator.

performance of IFCI through a simulation study in Section 6 and a real data application in Section 7.

2 Preliminaries

Let $G = (V, E)$ be a graph with vertex set V and edge set E . We only consider graphs that are *simple* (i.e., there is at most one edge between any pair of nodes) and free of self-loops (i.e., each edge joins two distinct nodes). We allow three types of edge marks (head, tail and circle) and six types of edges: directed (\rightarrow), bi-directed (\leftrightarrow), undirected ($-$), nondirected ($\circ\circ$), partially undirected ($\circ-$), and partially directed ($\circ\rightarrow$). A star \star denotes an arbitrary mark on an edge; e.g., $\star\rightarrow$ represents an edge of type \rightarrow , \leftrightarrow , or $\circ\rightarrow$ in the graph.

Our terminology follows standard conventions in graphical modeling (cf. Maathuis et al., 2019). In particular, a graph G is directed (or undirected) if it contains only directed (or only undirected) edges. A mixed graph may contain directed, bi-directed or undirected edges. The *skeleton* $\text{skel}(G)$ is the undirected graph with the same adjacencies as G . A *path* is a sequence of distinct vertices, where each pair of consecutive vertices is *adjacent*, i.e., linked by an edge. A path of *length* n has $n + 1$ vertices (i.e., n edges). A *directed path* is a path along directed edges following the arrowheads. Adding a directed edge back to the first node gives a *directed cycle*. A *directed acyclic graph (DAG)* is a directed graph without directed cycles. If a graph G contains the edge $k \rightarrow j$, then k is a *parent* of its *child* j . If it contains a directed path $k \rightarrow \dots \rightarrow j$, then k is an *ancestor* of its *descendant* j . The sets of parents, children, ancestors and descendants of j are denoted $\text{pa}(G, j)$, $\text{ch}(G, j)$, $\text{an}(G, j)$ and $\text{de}(G, j)$, respectively. We allow trivial paths, so that $j \in \text{an}(G, j)$ and $j \in \text{de}(G, j)$, but $j \notin \text{pa}(G, j)$ and $j \notin \text{ch}(G, j)$ as we exclude self-loops. A triple of vertices (i, j, k) is *unshielded* if j is adjacent to both i and k , but i and k are not adjacent. A non-endpoint vertex j on a path π is a *collider* on the path if the edges preceding and succeeding it both have arrowheads at j . Otherwise, j is a *non-collider* on π . A *v-structure* is an unshielded triple (i, j, k) with j as collider. The *neighborhood* $\text{adj}(G, i)$ is comprised of all nodes j adjacent to i in G . Its size $|\text{adj}(G, i)|$ is the *degree* of i . The maximal degree of any vertex is denoted by $d_{\max}(G)$. When clear from the context, we will drop the indication of the graph G , writing, e.g., d_{\max} or $\text{an}(i)$ only.

Consider a DAG G whose vertex set is partitioned as $V = X \cup L \cup Z$, where X indexes observed random variables, L indexes latent variables and Z indexes selection variables. As shown by Richardson and Spirtes (2002), G can be transformed into a unique maximal ancestral graph (MAG) G^* with vertex set X such that G^* retains the m -separation properties in G . The notion of m -separation, defined below, generalizes d -separation to MAGs. An ancestral graph is a mixed graph that contains no directed cycles or almost directed cycles (i.e., cycles formed by a directed path and a bidirected edge), and no subgraph of the type $i - j \leftrightarrow k$. Let $\text{un}(G)$ be the set of vertices in G that have no parents and are also not incident to a bidirected edge. Then in an ancestral graph, $\text{un}(G)$ induces an undirected subgraph that contains all undirected edges of G . An ancestral graph is a MAG if two vertices are non-adjacent only if they can be m -separated, i.e., all paths between them can be blocked in the following sense.

Definition 1 (m -separation). *A set Y blocks a path π in an ancestral graph if and only if:*

1. π contains a triplet (i, j, k) such that j is a non-collider on this path and $j \in Y$; or
2. π contains a v-structure $i \star \rightarrow j \leftarrow \star k$ such that $j \notin Y$ and no descendant of j is in Y .

If a path π from vertex i to vertex j is not blocked by Y , then π is also said to m -connect i and j given Y . If Y blocks every path between i and j , then i and j are m -separated given Y .

If i and j are m -separated by set S , we say S is a m -separator of i, j . Moreover, we say S is *minimal* if it has the smallest cardinality among all m -separators of i, j . The MAGs that have the same set of m -separation relations form a Markov equivalence class. We denote the Markov equivalence class of G^* as $[G^*]$. We say an edge mark is *invariant* in $[G^*]$ if it is the same in all members of $[G^*]$. The Markov equivalence class can be represented by a

partial ancestral graph (PAG), H , with three types of edge marks (head, tail and circle) that has the same adjacencies as G^* , and each non-circle edge mark in H is an invariant mark in $[G^*]$. For a given MAG, there may be more than one PAG that represents its Markov equivalence class. However, there is a unique PAG that is *maximally informative* in the sense that every non-circle edge mark is invariant, and every circle edge mark is variant. Alternatively, PAGs can be characterized as in Definition 1 in the Supplementary Material.

Given a vertex set V , a formal conditional independence statement is a triple denoted $A \perp\!\!\!\perp B | C$, where $A, B, C \subset V$ are non-empty and pairwise disjoint. The independence model defined by a MAG G , denoted $\mathcal{I}(G)$, is the set of formal conditional independence statements $A \perp\!\!\!\perp B | C$ for which A and B are m -separated by C in G . A probability distribution P obeys the model $\mathcal{I}(G)$ if all formal statements in $\mathcal{I}(G)$ are also probabilistic conditional independences in P . Such a distribution P is *faithful* to G if the conditional independence relations in P are exactly the same as $\mathcal{I}(G)$. If the distribution P over $X \cup L \cup Z$ is faithful to a DAG, and G is the MAG obtained by conditioning on Z and marginalizing L , then the absence of an edge between i and j in G implies that there exists some set $Y \subseteq X \setminus \{i, j\}$ such that $i \perp\!\!\!\perp j | Y \cup Z$, and the presence of an edge between i and j implies $i \not\perp\!\!\!\perp j | Y \cup Z$ for all $Y \subseteq X \setminus \{i, j\}$.

3 Local Separation in Large Random Graphs

3.1 Local separation and local paths

Our algorithm, presented in Section 4, is based on a *local separation property* that holds for many common networks. The property yields that short m -connecting paths between non-adjacent nodes can be blocked by small sets. A sufficient condition for the local separation property is the *local path property*, which involves a length and a path count parameter. These will be specified later for specific graphs.

Definition 2 ((η, γ) -local path property). *Let $\eta, \gamma \geq 1$ be integers. An undirected graph G satisfies the (η, γ) -local path property if for any two non-adjacent nodes, there are at most η paths between them with length no longer than γ .*

While it does not restrict the total number of paths, the (η, γ) -local path property implies that the number of short paths between non-adjacent nodes is bounded. Many random graph processes generate sequences of undirected graphs with increasing vertex set size p that (for process-specific η and γ) satisfy the (η, γ) -local-path property with probability tending to 1 as $p \rightarrow \infty$. Examples include Erdős-Renyi graphs (Bollobás and Béla, 2001; Anandkumar et al., 2011), power-law random graphs with strongly finite mean (Chung and Lu, 2006; Dembo and Montanari, 2010; Dommers et al., 2010), and Δ -regular random graphs (McKay et al., 2004). Surprisingly, in all these cases, the constants can be chosen as $\eta = 2$ and $\gamma = O(\log p)$.

Local separation in undirected graphs does not naturally extend to directed and mixed graphs, since m -separation is not implied by undirected graph separation. To overcome this issue, Sondhi and Shojaie (2019) consider a directed “local separator” between two nodes as the smallest set that blocks all short d -connecting paths between them. However, this “local separator” may unblock a large number of long d -connecting paths (see Figure 2). This is particularly problematic when edges amongst “local separator” nodes form dense structures. As a consequence, consistency of rPC requires strong assumptions on the data-generating distributions (under which the “local separators” act like true separators). In this work, we mitigate this limitation by focusing instead on subgraphs induced by nodes on short paths.

Definition 3 (Local graph). *For a graph $G = (V, E)$ and two nodes $i, j \in V$, let $P(G, i, j)$ be the set of all paths between i and j , and let $P_\gamma(G, i, j)$ be the set of those that are not longer than γ . The γ -local graph of $\{i, j\}$, denoted $G_\gamma(i, j)$, is the subgraph of G induced by the set $V_\gamma(i, j) = \{v \in V : v \in \pi \text{ for some } \pi \in P_\gamma(G, i, j)\}$.*

The motivation for our definition is that subgraphs better capture causal relations than subsets of paths. Moreover, m -separators in local graphs are interpretable.

Definition 4 (γ -local-graph separator). *Let i, j be two nodes in a MAG $G = (V, E)$. A γ -local-graph separator of (i, j) is a subset $S \subset V_\gamma(i, j)$ that m -separates i and j in $G_\gamma(i, j)$.*

A local-graph separator is a genuine m -separator in the subgraph: It blocks not only short, but also long paths in the local graph; see Figure 2. However, a set that m -separates i, j in $G_\gamma(i, j)$ does not necessarily m -separate them in G (see Figure 1). Hence, local-graph separations are not necessarily reflected in the independence model $\mathcal{I}(G)$. Nevertheless, the next result shows the existence of local-graph separators is equivalent to absence of edges.

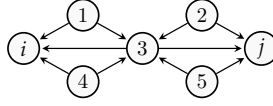


Figure 2: A graph G with $G = G_\gamma(i, j)$ for $\gamma = 3$; every node lies on a path of length at most three between i and j . The set $\{2, 3, 5\}$ is a γ -local-graph separator. In contrast, the definition of Sondhi and Shojaie (2019) makes the set $\{3\}$ a γ -“local separator” of (i, j) , although there are 4 “local but not short” paths (e.g., $i - 1 - 3 - 2 - j$) that are d -connected given $\{3\}$.

Lemma 1. *Let $G = (V, E)$ be a MAG, and let $\gamma \geq 1$ be any integer. Two nodes i, j are non-adjacent in G if and only if they are γ -local-graph separated by some set S_γ .*

Proof. By definition of MAGs, nodes i, j are non-adjacent in G if and only if there exists a set S that blocks all paths between i, j in G . If such a set exists, we write $S_\gamma = S \cap V_\gamma(i, j)$. Since $S \setminus S_\gamma$ is disjoint from $V_\gamma(i, j)$, all paths between i and j in the subgraph $G_\gamma(i, j)$ must be blocked by S_γ , and hence S_γ is a local separator. The other direction is trivial. \square

Though local-graph separators might be less informative than m -separators in the full graph, they usually have bounded size even in graphs with unbounded node degrees. Local separators can be useful in such cases, as the minimal m -separators in the full graphs might be large.

3.2 Graphs with small local-graph separators

The computational and sample complexities of PC and FCI algorithms depend on the maximum size of m -separators in the underlying graph. The applicability of the algorithms is thus limited to settings where the neighborhood-based D-SEP sets are all small. However, this does usually not hold in the presence of nodes with large degree (cf. Appendix B), which are common to many real-world networks. Nevertheless, such networks are often still sparse, in the sense of having small γ -local-graph separators. The algorithm proposed in this paper exploits this weaker notion of sparsity to offer sample and computational complexities that depend only on the maximum size of γ -local-graph separators, i.e., on

$$L(G, \gamma) = \max_{(i,j) \notin E} \min_{S \in \mathcal{S}_\gamma(i,j)} |S|,$$

where $\mathcal{S}_\gamma(i, j)$ is the set of all γ -local separators of nodes i, j in a mixed graph $G = (V, E)$.

If a DAG G has maximal in-degree at most $\Delta > 0$, then for arbitrary $\gamma \in \mathbb{N}$, it holds that $L(G, \gamma) \leq \Delta$. We next show that a similar upper bound holds more generally, as long as the DAG satisfies the local-path property, which allows for potentially unbounded node degrees.

Lemma 2. *If the skeleton of a DAG G satisfies the (η, γ) -local path property, then it holds that $L(G, \gamma) \leq \eta$.*

Proof. Fix any non-adjacent nodes i and j . Since G is acyclic, two nodes cannot be ancestors of each other in G or any subgraph. Without loss of generality, suppose $i \notin \text{an}(G, j)$, and let $S = \text{pa}(G_\gamma(i, j), i)$. Then paths between i and j in graph $G_\gamma(i, j)$ either have a non-collider included in $\text{pa}(G_\gamma(i, j), i)$, or have a collider that is not in $\text{pa}(G_\gamma(i, j), i)$. Thus, $\text{pa}(G_\gamma(i, j), i)$ is a d -separator. Since $G_\gamma(i, j)$ is induced by $P_\gamma(G, i, j)$, for each $v \in \text{ne}(G_\gamma(i, j), i)$, the edge (i, v) must lie on at least one short path between i and j . Therefore, $\eta \geq |\text{ne}(G_\gamma(i, j), i)| \geq |S|$. \square

Lemma 2 suggests that in many large random DAGs, the maximum node-degree of the local-path graph can be small while the maximum node-degree may be large. As a corollary to the construction we employed in the proof, the “approximation” of rPC in Sondhi and Shojaie (2019) is in fact an exact algorithm if the local path property holds (see Corollary 1).

The problem is more complicated for MAGs, which may have large minimal separators even with bounded degree (with bidirected edges m -separation of non-adjacent nodes generally requires consideration of non-neighboring nodes). Thus, compared with PC, the FCI theory requires an additional assumption on the size of possible d -separation sets. The theory for RFCI imposes a similar limit on the size of separators in the initial step (Colombo et al., 2012). The FCI+ theory exploits an assumption of bounded node degree to avoid additional assumptions on the size of bidirected components (Claassen et al., 2013). However, these results either prohibit the existence of generic hub nodes with large degrees or have sub-par sample and computational complexities. In contrast, the size of minimal

local-separation sets is determined by short paths in $G_\gamma(i, j)$. Thus, by utilizing local-graph separators, and under the additional assumptions discussed in Section 5, our framework achieves improved computational and sample complexity. Next we show that as long as the skeleton of a MAG has small number of short paths, the size of the local-separators is controlled:

Lemma 3. *If the skeleton of a MAG G satisfies the (η, γ) -local path property with $\eta \leq 3$, then $L(G, \gamma) \leq \eta$.*

Proof. This lemma is proved by enumeration of all possible graph configurations. Details are given in Appendix A. \square

Lemma 3 covers most common random graphs. For instance, for Erdős-Renyi graphs, power-law graphs with strongly finite mean, and Δ -regular graphs, it holds with $\eta \leq 2$. As we discuss in Section 4, for these graphs, we only need to search for separators of size up to 2.

Our next result shows that we can further reduce the size of separator by restricting focus on pairs of nodes in *local Markov blankets*. The *Markov blanket* of node i in a MAG G , denoted $\text{mb}(G, i)$, is the minimal set of vertices that separates i from all other vertices. Concretely, it is the union of vertices connecting to i through either an edge, or a collider path (i.e., a path on which all non-endpoints are colliders). The γ -local Markov blanket $\text{mb}_\gamma(G, i)$ is the union of vertices connecting to i through either an edge or a collider path of length at most γ .

Lemma 4. *Let $G = (V, E)$ be a MAG, and define*

$$L^{mb}(G, \gamma) = \max_{(i,j) \notin E, i \in \text{mb}_\gamma(G, j)} \min_{S \in \mathcal{S}_\gamma(i, j)} |S|.$$

If the skeleton of G satisfies the (η, γ) -local path property with $\eta \leq 4$, then

$$L^{mb}(G, \gamma) \leq \max(0, \eta - 1).$$

Proof. Suppose $i \notin \text{adj}(G, j)$ but $i \in \text{mb}_\gamma(G, j)$. Then i and j must be connected via a collider path π . There must be a node on π , call it u , that is not ancestral to i and j , because π would otherwise prevent m -separation of i and j , which contradicts G being a MAG. Let $G_\gamma^u(i, j)$ be the subgraph of $G_\gamma(i, j)$ induced by the complement of u . Every minimal separator of (i, j) in $G_\gamma^u(i, j)$ also minimally separates i and j in $G_\gamma(i, j)$ (see, e.g., van der Zander and Liskiewicz, 2019). It is easy to see that $G_\gamma^u(i, j)$ has at most $\eta - 1$ many short paths between i and j . Hence, the result follows from Lemma 3. \square

More generally, our framework accommodates hybrid graphs, consisting of a “global” graph with small maximal degree, and a “local” graph with bounded local-paths, paralleling the class of undirected hybrid graphs defined in Chung and Lu (2006). As a concrete example, the Watts-Strogatz (or small-world) graph consists of the union of a d -dimensional regular graph and an Erdős-Renyi random graph (Watts and Strogatz, 1998).

Theorem 1. *Let $G = (V, E)$ be a MAG. For any two non-adjacent nodes i and j , let M_{ij} be the set of nodes that do not lie on any path in $P(G, i, j)$ that uses a bidirected edge. Suppose for each pair of non-adjacent nodes i, j , there exists a set $M \subseteq M_{ij}$ such that the subgraph of G induced by $M \cup \{i, j\}$ has node-degree no larger than Δ , and the subgraph of G induced by $V \setminus M$ satisfies the local path property with some $\eta_0 \leq 3$ and some γ . Let $\eta = \eta_0 + \Delta$. The following statements hold,*

$$L(G, \gamma) \leq \eta \quad \text{and} \quad L^{mb}(G, \gamma) \leq \max(0, \eta - 1).$$

Proof. Let i, j be non-adjacent nodes in G . Without loss of generality, let $i \notin \text{an}(G, j)$. Let G^1 and G^2 be the subgraphs induced by $M \cup \{i, j\}$ and $V \setminus M$, respectively. Let $S^1 = \text{pa}(G^1, i)$, and let S^2 be a γ -local-graph separator of (i, j) in G^2 . We have $P(G, i, j) = P(G^1, i, j) \sqcup P(G^2, i, j)$ where \sqcup stands for disjoint union. Thus, $S^1 \sqcup S^2$ is a γ -local-graph separator of (i, j) . By Lemma 3, $|S^1| + |S^2| \leq \Delta + \eta_0$. Lemma 4 gives the Markov blanket result. \square

4 A Local FCI Algorithm (IFCI)

In this section, we propose a novel algorithm that discovers absent edges by searching for local-graph separators, as defined in Section 3.

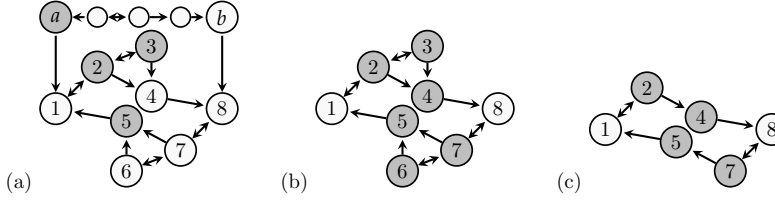


Figure 3: Search strategies of FCI and IFCI: (a) True G , (b) local-graph $G_4(1, 8)$, (c) local-graph $G_3(1, 8)$. Search pools $J_{\text{FCI}}(1, 8)$, $J_4(1, 8)$ and $J_3(1, 8)$ are shaded. FCI discovers the separator $\{a, 2, 3, 5\}$ in G (differs from minimal separator $\{a, 4, 5\}$). For both $\gamma = 3, 4$, IFCI discovers the local-graph separator $\{4, 5\}$ (small but only correct in the local graph). Note that FCI cannot be early-stopped at reach level 2 even if we ignore the path $(1, a, \dots, b, 8)$.

4.1 IFCI

To learn a MAG $G = (V, E)$, PC/FCI adopt the following strategy. Starting with a complete undirected graph C , they first search for separating sets of size $\ell = 0$: If two nodes are independent given a set of size 0 (i.e., marginally independent), the corresponding edge in C is removed. Iteratively increasing the value of ℓ by one, the algorithm visits all pairs (i, j) adjacent in C and searches amongst all sets $S \subseteq J(i, j, C)$ with $|S| = \ell$, where $J(i, j, C) \subseteq V \setminus \{i, j\}$ is a current *search pool*. If a conditional independence $i \perp\!\!\!\perp j | S$ is found, the edge $i - j$ is removed from C . The algorithm stops when ℓ exceeds the maximum size of the sets in the search pool. (In rPC, the iterations are stopped early at a specified level for ℓ .) The value of ℓ at termination is the *reach level*, denoted m_{reach} . With a conditional independence oracle, PC terminates at $m_{\text{reach}}(\text{PC}) \leq d_{\text{max}} - 1$, where d_{max} is the maximum node degree; the reach level of the second step of FCI is the maximum size of p-D-SEP sets.

Our IFCI algorithm follows a similar strategy but with two key differences. The first difference is the construction of the search pool, $J(i, j, C)$. Given a working skeleton C that is a supergraph of $\text{skel}(G)$, a construction of $J(i, j, C)$ is valid if each pair of non-adjacent nodes (i, j) is separated by some subset of $J(i, j, C)$. PC/FCI adopt a neighborhood-based strategy: PC uses $J_{\text{PC}}(i, j, C) = (\text{adj}(i, C) \cup \text{adj}(j, C)) \setminus \{i, j\}$, and FCI uses J_{PC} in its first step and $J_{\text{FCI}}(i, j, C) = \text{p-D-SEP}(i, j)$ in its second step. In contrast, inspired by the local separation property, our IFCI algorithm adopts a local-graph-based strategy, in which we form an alternative search pool that is guaranteed to contain a local separator by including the nodes that are *close* to both i and j . Figure 3 exemplifies the difference between neighborhood-based and local-graph-based searches. More concretely, let $D_G(i, j) = \min_{\pi \in P(G, i, j)} |\pi|$ be the shortest-undirected-path distance between nodes i and j in G , with $D_G(i, j) = \infty$ if $P(G, u, v) = \emptyset$. Writing C_{-ij} for the working skeleton C with edge $i - j$ removed, we define

$$J_\gamma(i, j, C) = \{k \in V \setminus \{i, j\} : D_{C_{-ij}}(i, k) + D_{C_{-ij}}(j, k) \leq \gamma\}. \quad (1)$$

While otherwise distinct, the idea of searching among nodes that lies on connecting paths is related to the path modification of FCI in FCI_{path} (Colombo and Maathuis, 2014), which uses a different search pool, $J_{\text{FCI}_{\text{path}}}(i, j, C) = J_{\text{FCI}}(i, j, C) \cap J_p(i, j, C)$. The following lemma shows that $J_\gamma(i, j, C)$ is a superset of $V_\gamma(i, j)$ from Definition 3 and is hence a valid search pool.

Lemma 5. *Let G be a MAG, and let C be a super-graph of $\text{skel}(G)$. Two nodes i, j are non-adjacent in G if and only if they are γ -local-graph separated by a subset of $J_\gamma(i, j, C)$.*

The second innovation in our approach lies in its termination criterion. The complexities of PC and FCI are determined by their reach levels m_{reach} , which scale with the maximum degree d_{max} of the graph. As a result, these values can be very large if the graph includes hub nodes. In particular, when considering sequences of structure learning problems where a few nodes are allowed to have $O(p)$ many neighbors, PC and FCI (and also FCI+) cannot terminate in polynomial time. Our approach offers a strategy to circumvent this problem by early termination when searching on local graphs. Indeed, sparse graphs may still satisfy the conditions in Theorem 1 for bounded η . The reach level of our local-graph-based approach is then at most η , so $O(1)$. Therefore, through its focus on local graphs, our IFCI algorithm may enjoy polynomial-time complexity even in graphs with hub nodes—settings that become problematic for PC and FCI. We emphasize that an ad hoc early stopping (or “anytime”) version of PC and FCI avoids the computational issue (Spirites, 2001) but will generally result in false discoveries. Indeed, even if the conditions in Theorem 1 hold, the smallest neighborhood-based D-SEP set is not necessarily small; compare Figure 3.

Our IFCI proposal is summarized in Algorithm 1. Starting with a complete graph C and level $\ell = 0$, IFCI traverses every edge (i, j) and searches for a conditional independence

Algorithm 1: IFCI

Input : Tests of conditional independences $i \perp\!\!\!\perp j|S$,
maximum separating set size η , locality parameter γ .
Output: A partial ancestral graph C
 $C, C_{\text{old}} \leftarrow$ complete undirected graph over $[p]$;
Initialize SEP $\leftarrow \emptyset$ and $\ell \leftarrow -1$;
repeat
 $\ell \leftarrow \ell + 1$;
 repeat
 Select a (new) ordered pair of nodes (i, j) that are adjacent in C ;
 repeat
 Choose a (new) $S \subseteq J_\gamma(i, j, C_{\text{old}})$ with $|S| = \ell$;
 if $i \perp\!\!\!\perp j|S$ **then** Delete edge (i, j) from C , and record $\text{SEP}(i, j) \leftarrow S$;
 until (i, j) is deleted or all subsets of $J_\gamma(i, j, C_{\text{old}})$ with size ℓ are checked;
 until all ordered pairs of (i, j) has been checked;
 $C_{\text{old}} \leftarrow C$;
until $\ell > \eta$;
Orient edges in C using the SEP sets, by the modified rules in Section 4.3;
return A PAG C .

$i \perp\!\!\!\perp j|S$ given subsets $S \in J_\gamma(i, j, C)$ of size $|S| = \ell$. If a conditional independence is found the edge is removed from C . The level ℓ is increased after checking all edges, and the algorithm terminates when ℓ hits the reach level $m_{\text{reach}} = \eta$, which is picked in advance with a view towards potential underlying graph structure (similar to how node degrees are bounded in other algorithms). Throughout the search, we keep track of the shortest-path-distances between nodes, but only update them after completing the ℓ -th level. This makes the algorithm *order-independent*, i.e., the output does not depend on the order in which edges are tested (see, e.g., Colombo and Maathuis, 2014).

4.2 Tuning parameters

Given Lemma 5, γ acts as a tuning parameter that controls the breadth of the search in our algorithm. Theoretically, γ should be small enough such that the underlying graph G has small γ -local-graph separators, yet large enough such that paths not contained in G_γ contribute little to total effects in the graphical model. Theorem 1 notes that many random graphs satisfy $L(G, \gamma) \leq \eta$ with $\gamma = O(\log p)$ with high probability as the number of nodes $p \rightarrow \infty$. Due to this fact, our later analysis allows (but does not require) γ to grow with p , in which case distributional conditions may be weakened for larger graphs. We note that in our later simulations IFCI terminates early, and its performance is rather insensitive to our choice of γ , see Section 4 of the Supplementary Material.

The maximum size of separating sets, η , is a tuning parameter that controls the depth of the search and allows IFCI to terminate at smaller levels than PC/FCI. Choosing η is akin to an a priori choice of the maximum node degree in other algorithms, recall Theorem 1.

4.3 Orientation rules

After inferring the skeleton using conditional independence tests, we orient as many edges as possible to obtain a PAG representation of the Markov equivalence class of MAGs. Given the undirected skeleton of the true MAG and a collection of minimal separators, the orientation procedure proposed in Zhang (2008) applies eleven deterministic rules to obtain the maximally informative PAG. In other words, the population version of FCI is sound (i.e., never returns a wrong result) and complete (i.e., the output is maximally informative in the sense of discovering all causal relations common to the graphs in the equivalence class). However, these properties are *not* guaranteed if we apply the rules directly with local-separation, because the local separators are usually not m -separators.

Surprisingly, however, soundness under local-separation can be achieved with only a single change to Zhang’s Rule \mathcal{R}_4 , which pertains to *discriminating paths*. Furthermore, completeness can be achieved under an additional condition on these discriminating paths. A path between i and j , $\pi = (i, \dots, x, y, j)$, is a discriminating path for y if π includes at least three edges; y is adjacent to j on π ; i is not adjacent to j ; and every vertex between i and y is a collider on π as well as a parent of j . An example of the failure of the unmodified discrimination path rule (Rule \mathcal{R}_4) is given in Figure 4. The original (Zhang, 2008) and the modified versions may be contrasted as follows:

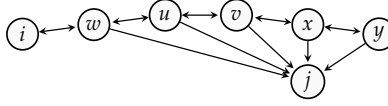


Figure 4: Nodes i and j are m -separated given $\{w, u, v, x, y\}$ and all other non-adjacent pairs are marginally m -separated. There is a discriminating path (i, w, u, v, x, y, j) for y . In FCI, the edge $y \rightarrow j$ is oriented correctly. For $\gamma = 5$, the γ -local separator of (i, j) is $\{w, u, v, x\}$, with which the discriminating path rule outputs $y \leftrightarrow j$, which is inconsistent with the truth.

\mathcal{R}_4 : If π is a discriminating path between i and j for y , and $y \circ \star j$, then if $y \in S(i, j)$, orient $y \circ \star j$ as $y \rightarrow j$; otherwise orient the triple (x, y, j) as $x \leftrightarrow y \leftrightarrow j$.

\mathcal{R}'_4 : If π is a discriminating path between i and j for y , and $y \circ \star j$, then if $v \in S(i, j)$, orient $y \circ \star j$ as $y \rightarrow j$; if $y \notin S(i, j)$ and all vertices in π are contained in the γ -local-graph of (i, j) , then orient (x, y, j) as $x \leftrightarrow y \leftrightarrow j$; otherwise orient $y \circ \star j$ as $y \leftrightarrow j$.

Rule \mathcal{R}'_4 avoids wrong decisions when local-graph separators do not provide enough information. The original and modified rules give the same output under the following condition.

Assumption 1 (Local discriminating paths). *Let G be a MAG and γ be an integer. Denote $\Pi^D(G, i, j, y)$ as the set of discriminating paths between i and j for y in G . If $\Pi^D(G, i, j, y) \neq \emptyset$ for the triple (i, j, y) , then there exists $\pi \in \Pi^D(G, i, j, y)$ such that $\pi \subset G_\gamma(i, j)$.*

In the next lemma we show soundness and completeness of population lFCI.

Lemma 6. *Let G be a MAG. Let the lFCI parameters η and γ be integers such that $\gamma > 2$ and $L(G, \gamma) \leq \eta$. Then with a local-graph separation oracle, lFCI outputs a PAG for $[G]$. If in addition Assumption 1 holds, then the lFCI output is the maximally informative PAG.*

Proof. By Lemma 1, the output of the skeleton step is correct. In FCI, Zhang's orientation rules \mathcal{R}_0 (unshielded triple rule) and \mathcal{R}_4 (discriminating path rule) introduce arrowheads using the separation sets, whereas the rest of the rules, \mathcal{R}_1 – \mathcal{R}_3 and \mathcal{R}_5 – \mathcal{R}_{10} , only depend on the results of \mathcal{R}_0 and \mathcal{R}_4 . Therefore, the orientation phase is sound if all arrowheads introduced by \mathcal{R}_0 and \mathcal{R}_4 are correct, and complete if \mathcal{R}_0 and \mathcal{R}_4 introduce as many arrowheads as possible. For details of the rules, see Zhang (2008).

First we consider \mathcal{R}_0 , which orients an unshielded triple (i, j, k) into a v-structure if j is not in the separator for (i, k) . In lFCI, if j is not in the γ -local separator, then (i, j, k) must be a marginally blocked path in both G and $G_\gamma(i, k)$. Thus, \mathcal{R}_0 produces the same output using local- and full-graph-separators. Next we show \mathcal{R}'_4 is sound. Indeed, if π is a discriminating path between i, j for y and $y \in S_\gamma(i, j)$, then the last edge on π must be oriented as $y \rightarrow j$ to avoid unblocking π . If $y \notin S_\gamma(i, j)$ and π is contained in the local-graph, then \mathcal{R}'_4 is the same as \mathcal{R}_4 in $G_\gamma(i, j)$; otherwise, \mathcal{R}'_4 simply avoids making wrong decisions. We conclude that by Theorem 1 of Zhang (2008), the orientation phase of lFCI using local-separators is sound.

Under the additional condition, if (i, j, y) can be oriented using a full-graph separator by \mathcal{R}_4 , then there is a discriminating path in $G_\gamma(i, j)$ such that the same orientation is made by \mathcal{R}'_4 . Therefore, the lFCI output is identical to that of FCI, which is maximally informative. \square

4.4 Computational complexity

As discussed in Section 4.1, the computational advantages of lFCI over FCI, RFCI and FCI+ stem from two key differences: (i) the use of a local-graph-based strategy (J_γ) instead of the neighborhood-based strategy (J_{FCI}); and (ii) searching up to sets of size η . As a result, lFCI achieves computational complexity $O(p^{\eta+2})$, which is the same as that of rPC (Sondhi and Shojaie, 2019). In contrast, the worst case computational complexity of FCI is exponential and FCI+ has computational complexity $O(p^{d_{\max}+2})$. Though FCI+ offers polynomial complexity when d_{\max} is bounded (Claassen et al., 2013), it becomes inefficient in the setting of power-law graphs with highly connected hub nodes, when $d_{\max} = O(p^a)$ for some $a > 0$ (Molloy and Reed, 1995). For these graphs, FCI+ offers exponential complexity $O(p^{p^{a+2}})$, compared with $O(p^4)$ for lFCI.

4.5 Initialization with Moral Graph

Following the observation from Lemma 4, in Algorithm 2 we propose a modified version of lFCI that utilizes local Markov blankets for improved computational and sample complex-

Algorithm 2: IFCI_{mb}: IFCI with moral graph step

Input : Tests of conditional independences $i \perp\!\!\!\perp j|S$,
maximum separating set size η , locality parameter γ .
Output: A partial ancestral graph C
 $C \leftarrow$ estimated local moral graph;
Run the edge removal loop in Algorithm 1 for search set size $l = 1, \dots, \eta - 1$;
Orient edges in C using the SEP sets, by the modified rules in Section 4.3;
return A PAG C .

ities. Concretely, instead of starting with a complete graph C , Algorithm 2 starts with an estimated *local moral graph*.

The moral graph of a MAG G is the undirected graph in which two nodes i, j are adjacent whenever one node is in the G -Markov blanket of the other, say $j \in \text{mb}(G, i)$. Accordingly, the local moral graph is the undirected graph obtained by taking instead the γ -local Markov blankets, $\text{mb}_\gamma(G, i)$. For large enough γ , these two notions coincide as the local moral graph differs from the moral graph only if the shortest path between two nodes is longer than γ and only includes bidirected edges. This is unlikely in large common random graphs if we allow γ to increase with p ; see Section 6 of the Supplementary Material. Consequently, we simply employ the moral graph, which in the models we treat later can be estimated by the support of the inverse covariance matrix. In our simulation study, we used score matching to estimate the precision matrix in high dimensions (Lin et al., 2016; Yu et al., 2019), which here coincides with the SCIO algorithm (Liu and Luo, 2015).

Initializing C as an estimated moral graph may significantly recude the size of the search pools $J_\gamma(i, j, C)$. Moreover, this additional step allows Algorithm 2 to terminate at level $\eta - 1$ instead of η (Lemma 4). For Erdős-Renyi graphs, power-law graphs with strong finite mean, and Δ -regular graphs, the algorithm can then stop after checking separating sets of size 0 and 1 only. However, these improvements require slightly more restrictive conditions in theoretical analysis (see Appendix A). We will explore the performance of Algorithm 2 in Section 6.

5 Consistency of the IFCI Algorithm

In this section, we establish the consistency of our IFCI algorithm in high-dimensional settings, i.e., when the number of nodes in the graph is potentially larger than the available sample size. To this end, we first discuss in detail a set of assumptions under which IFCI is consistent. We focus on linear structural equation models with sub-Gaussian noise. Proofs are provided in Appendix A.

5.1 Linear Structural Equation Models

Let $G = (V, E)$ be a MAG with vertex set $V = \{1, \dots, p\}$. Let $W = (W_1, \dots, W_p)$ be an associated random vector. The linear structural equation model given by G assumes that W solves an equation system of the form

$$W = BW + \epsilon, \quad (2)$$

where $B = (\beta_{i,j}) \in \mathbb{R}^{p \times p}$ is a matrix of unknown parameters with $\beta_{ij} \neq 0$ only if $j \rightarrow i$ is an edge in G . The random vector $\epsilon = (\epsilon_1, \dots, \epsilon_p)$ is comprised of stochastic noise with positive definite covariance matrix $\text{Var}(\epsilon) = \Omega = (\omega_{i,j})$. It can be partitioned into two independent subvectors $\epsilon_{\text{un}(G)}$ and $\epsilon_{V \setminus \text{un}(G)}$. Here, $\epsilon_{\text{un}(G)}$ is assumed to satisfy the global Markov property for the undirected subgraph induced by the undirected part $\text{un}(G) \subseteq V$, and $\epsilon_{V \setminus \text{un}(G)}$ satisfies the global Markov property for the subgraph formed by the bidirected edges among nodes in $V \setminus \text{un}(G)$; compare, e.g., Drton and Richardson (2008). In particular, ϵ_i and ϵ_j are marginally independent when $i, j \notin \text{un}(G)$, and conditionally independent given all other errors when $i, j \in \text{un}(G)$. Consequently, the error covariance matrix Ω can be permuted into block-diagonal form with two blocks. One block has an inverse whose support is given by the undirected edges of G , and the other block has its support given by the bidirected edges of G (Richardson and Spirtes, 2002, Section 8).

Let I be the identity matrix. Since G is a MAG, it does not contain any directed cycles. Thus $I - B$ is invertible, and (2) has a unique solution W with covariance matrix

$$\Sigma := \text{Var}(W) = (I - B)^{-1} \Omega (I - B)^{-\top}. \quad (3)$$

Conditional independences in the linear SEM correspond exactly to zero *partial correlations*. For nodes i and j , and $S \subseteq V \setminus \{i, j\}$, the partial correlation of W_i and W_j given W_S is

$$\rho(i, j|S) = \Sigma(i, j|S) / \sqrt{\Sigma(i, i|S)\Sigma(j, j|S)},$$

where $\Sigma(i, j|S) = \Sigma(i, j) - \Sigma(i, S)\Sigma(S, S)^{-1}\Sigma(S, j)$. Given a sample of n independent observations generated from the distribution of W , the corresponding *sample partial correlations* $\widehat{\rho}(i, j|S)$ are obtained by replacing Σ by the sample covariance matrix $\widehat{\Sigma}_n$. In order to test $i \perp\!\!\!\perp j|S$ in a practical run of the IFCI algorithm, we test the vanishing of $\rho(i, j|S)$ and reject the conditional independence if $\sqrt{n - |S| - 3} |g(\widehat{\rho}(i, j|S))| > \Phi^{-1}(1 - \alpha_n/2)$, where $g(\rho) = \frac{1}{2} \log \left(\frac{1+\rho}{1-\rho} \right)$ is Fisher's z-transform, Φ is the normal cdf, and $\alpha_n \in (0, 1)$ is a significance level.

5.2 Consistency

As discussed in Section 3, our algorithm requires an assumption on the size of γ -local-graph separators.

Assumption 2 (Local-separation Property). *The MAG G satisfies $L(G, \gamma) \leq \eta$ for the IFCI parameters η and γ .*

As shown in Section 3, many common random graphs satisfy Assumption 2 with $\eta = O(1)$ and $\gamma = O(\log p)$ with high probability as the number of nodes $p \rightarrow \infty$. If the graph satisfies the requirements of Theorem 1, then Assumption 2 holds with $\eta = \eta_0 + \Delta$.

We also require an assumption on the covariance matrix to establish large sample consistency of estimated conditional correlations in high dimensions.

Assumption 3 (Covariance/precision matrix). *The random vector $W = (W_1, \dots, W_p)$ follows a linear SEM of the form (2), with sub-Gaussian errors ϵ . Moreover, the spectral norms of all $(\eta + 2) \times (\eta + 2)$ submatrices of its covariance matrix Σ are bounded as*

$$\max_{A \subseteq [p], |A| \leq \eta+2} (\|\Sigma_{A,A}\|, \|(\Sigma_{A,A})^{-1}\|) \leq M < \infty.$$

As in Sondhi and Shojaie (2019), we assume a faithfulness condition that is less restrictive than the λ -strong faithfulness assumption that appears, e.g., in Colombo et al. (2012).

Definition 5 ((η, λ) -strong-path-faithfulness). *Given $\eta > 0$ and $\lambda \in (0, 1)$, a distribution P is (η, λ) -strong-path-faithful to a MAG $G = (V, E)$ if both of the following conditions hold:*

- (i) $\min\{|\rho(i, j|S)| : (i, j) \in E, S \subset V \setminus \{i, j\}, |S| \leq \eta\} > \lambda$, and
- (ii) $\min\{|\rho(i, j|S)| : (i, j, S) \in N_G\} > \lambda$, where N_G is the set of triples (i, j, S) such that i and j are not adjacent, but for some $k \in V$, (i, j, k) is an unshielded triple, and i and j are not m -separated given S .

Assumption 4 (Path faithfulness and Markov property). *The joint distribution P of the random vector W is (η, λ) -strong-path-faithful to the MAG G with $\lambda = \Omega(n^{-c})$ for $c \in (0, 1/2)$.*

The next assumption captures the local point of view underlying our algorithm and posits small partial correlations given local separators.

Assumption 5 (Local partial correlation). *Let $\mathcal{S}_{\eta, \gamma}(i, j)$ denote the collection of γ -local-graph separators of (i, j) with size at most η . It holds that*

$$\max_{(i, j) \notin E} \min_{S \in \mathcal{S}_{\eta, \gamma}(i, j)} |\rho(i, j|S)| \leq \lambda.$$

As we now show this assumption holds under a directed β -walk-summability condition. This condition mirrors the walk-summable condition for undirected graphs, which holds for a large class of networks (Malioutov et al., 2006).

Assumption 6 (Directed β -summability). *The joint distribution P of the random vector W belongs to a linear SEM in the form (2), in which the weighted adjacency matrix B satisfies $\|B\| \leq \beta < 1$, where $\|\cdot\|$ denotes the spectral norm.*

If the norm of the error covariance matrix Ω is bounded, then directed β -summability implies Assumption 5. We state this in the following lemma, which is a slightly modified version of Lemma 2 in Sondhi and Shojaie (2019).

Lemma 7. *If Assumptions 2, 3, 4, 6 are satisfied, $\|\Omega\|$ is bounded, and γ is larger than some constant $\gamma^*(\eta, M, \lambda, \|\Omega\|)$, then Assumption 5 is also satisfied.*

To further justify Assumption 5, we conducted simulation studies (see Appendix B and Section SM5 of the Supplementary Material) which show that in a number of natural settings, Assumption 5 is likely to hold.

We now establish our main consistency result.

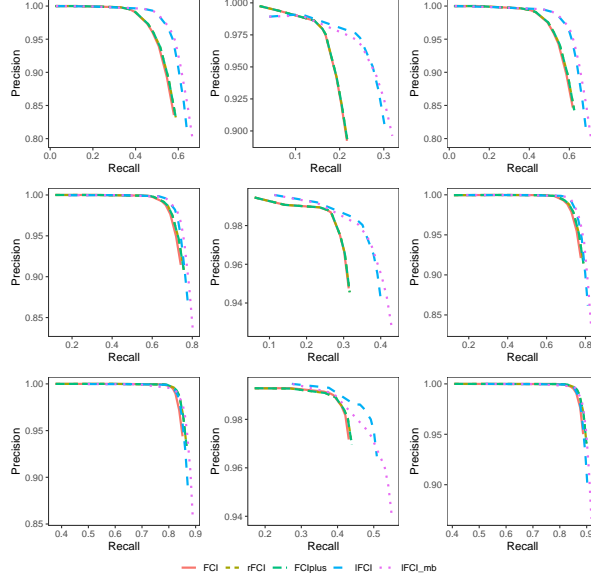


Figure 5: Precision-recall (PR) curves for graphs with $p = 100$ from Erdős-Renyi (left column), power-law (middle column), and Watts-Strogatz (right column) graphs based on $n = 100$ (top row), $n = 200$ (middle row), $n = 500$ (bottom row) samples.

Theorem 2. Suppose Assumptions 2, 3, 4, 5 hold, and $n = \Omega((\log p)^{1/(1-2c)})$ for $c \in (0, 1/2)$ from Assumption 4. Then there exists a sequence of significance levels $\alpha_n \rightarrow 0$ such that Algorithm 1 consistently learns a PAG for $[G]$ from an i.i.d. sample of size n . Moreover, if Assumption 1 holds, then the consistently learned PAG is maximally informative.

The sample complexity of lFCI established in Theorem 2 offers considerable improvement over the worst-case sample complexity of the FCI and rFCI algorithms for graphs with unbounded size of D-SEP sets and the FCI+ algorithm for graphs with large node degrees.

As a corollary, we also improve the theory of reduced PC (Sondhi and Shojaie, 2019) for DAG learning: we derive the correctness of reduced PC and its “approximate version” under the local path condition (Definition 2). The sample complexity is also improved by applying an alternative error propagation computation; see Appendix A for details.

Corollary 1. Suppose G is a DAG whose skeleton satisfies the (η, γ) -local path property. Under Assumptions 3, 4, 5 and assuming $n = \Omega((\log p)^{1/(1-2c)})$, there exists a sequence of significance levels $\alpha_n \rightarrow 0$ such that rPC and the approximate rPC both consistently learn the CPDAG of G from an i.i.d. sample of size n .

6 Numerical Experiments

We explore the performance of our algorithm on three types of graphs: Erdős-Renyi, power-law, and Watts-Strogatz graphs. Since generating general random MAGs is challenging, for each family, we generate DAGs with $p = |V| \in \{100, 200, 500\}$ nodes and average node degree 2 using the `igraph` library in R. Edge weights are drawn uniformly from $(-1, -0.1] \cup [0.1, 1)$, and $n = \{100, 200, 500\}$ observations are generated using the `rmvDAG` function in the `pcalg` library (Kalisch et al., 2012). We randomly choose $q = 0.2p$ nodes as latent variables, and the rest as observed. We include no selection variables.

We run FCI, rFCI, FCI+, lFCI, and the Markov blanket version of lFCI on the observed data, with thresholds $\alpha = \{10^{-20}, 10^{-10}, 10^{-5}, 10^{-4}, 0.5 \cdot 10^{-4}, 10^{-3}, 0.5 \cdot 10^{-3}, 10^{-2}\}$. The `pcalg` library is used for the existing methods. We run lFCI with $\eta = 2$ and $\gamma = \lceil \log p \rceil$. We repeat the experiment 200 times for each α . The maximum node degrees of Erdős-Renyi graphs and Watts-Strogatz graphs ranges from 7 to 9. The maximum node degrees of power-law graphs grow with p , with medians 41, 68 and 130.

The performance of the algorithms are evaluated using precision-recall curves with respect to skeletons in Figures 5–7. In all settings, Algorithm 1 and 2 offer improvement over existing methods in terms of larger area under curves. Though they sometimes have lower precision in the beginning of the curves, they offer better trade-offs for higher recall

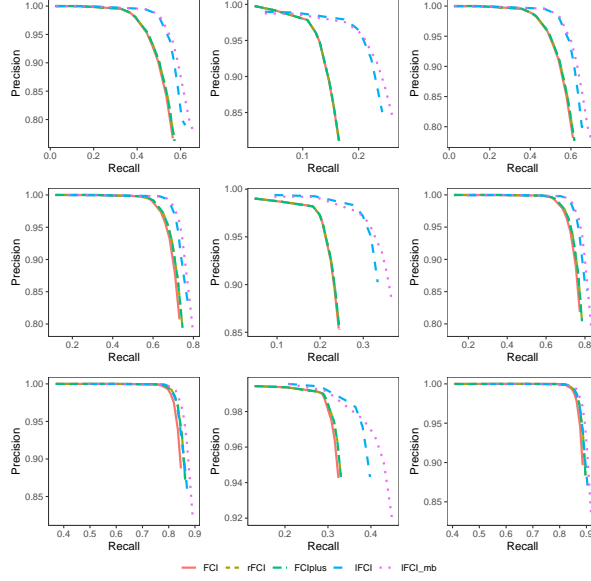


Figure 6: Precision-recall (PR) curves for graphs with $p = 200$ from Erdős-Renyi (left column), power-law (middle column), and Watts-Strogatz (right column) graphs based on $n = 100$ (top row), $n = 200$ (middle row), $n = 500$ (bottom row) samples.

values. The improvement is substantial in high-dimensional cases. For power-law graphs, Algorithm 1 and 2 are superior in both low- and high-dimensional settings.

We also compare the edge orientation performances by counting the average number of different edge marks between the outputs and the true maximally informative PAG. We only show comparison in the case of $n = 200$ and $\alpha = 10^{-4}$. Differences in edge marks are shown together with the Structural Hamming Distances (SHD) between output and truth in Figure 8. The performance of Algorithm 1 is on par with FCI/rFCI and superior to FCI+ in both low- and high-dimensional cases. Though Algorithm 2 performs better in the skeleton steps, the orientation steps are not as reliable in high-dimensional cases. A comparison of computational cost is presented in the Supplementary Material.

7 Application: Gene Regulatory Network Inference

We apply the IFCI algorithm to gene expression data from The Cancer Genome Atlas (TCGA) database (Cancer-Genome-Atlas-Research-Network, 2012). The dataset contains the gene expression levels measured by RNAseq for 20530 genes from $n = 551$ patients with prostate cancer. The aim of this application is to infer the regulatory network among the genes.

We construct a network of known gene regulatory relations among genes measured in TCGA with at least one known interaction in BIOGRID (Stark, 2006); this leaves us with a graph G^B with $p = 2478$ nodes. The graph G^B includes many disjoint subgraphs, of which only 10 subgraphs (denoted $G_i^B = (V_i^B, E_i^B)$, $i = 1, \dots, 10$) have more than 2 nodes; see Figure 9. Since BIOGRID represents gene regulatory relations in normal cells, G^B might not accurately capture the interactions in cancerous cells (Ideker and Krogan, 2012; Shojaie, 2021). We denote the true unobserved network in cancerous cells as G^T to underscore this difference.

In practice, the true graphs, $G_i^T = (V_i, E_i^T)$, are unknown. However, the clustering of nodes in G^T are expected to be similar to those in G^B . Thus, assuming that induced subgraphs of G^T over V_1^B, \dots, V_{10}^B are also disjoint, we use the PC algorithm to estimate the edge sets of G_i^T , $i = 1, \dots, 10$. Specifically, for each V_i , we run PC with different significance levels and choose the one that maximizes the eBIC score (Foygel and Drton, 2010). We denote the resulting CPDAGs as $\tilde{G}_i = (V_i, \tilde{E}_i)$. The skeleton of these graphs are shown in Figure 10. Figures 9 and 10 demonstrates the similarities and discrepancies between G^B and G^T .

To capture the situation in which researchers only have access to data from a subset of genes, we run the following experiment on each subgraph: We randomly sample a subset

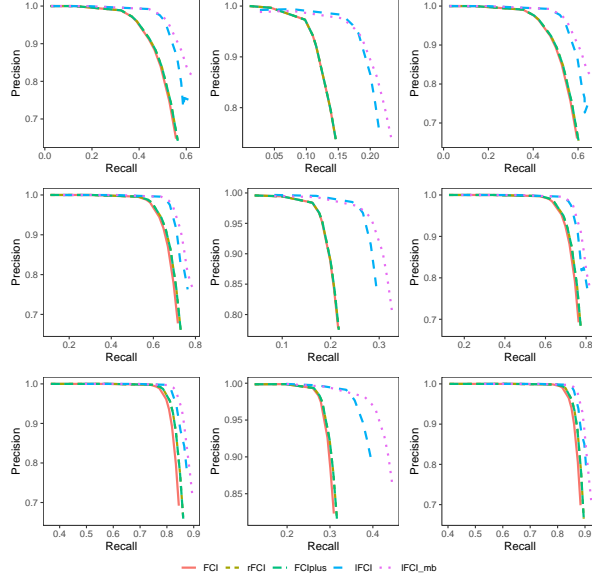


Figure 7: Precision-recall (PR) curves for graphs with $p = 500$ from Erdős-Renyi (left column), power-law (middle column), and Watts-Strogatz (right column) graphs based on $n = 100$ (top row), $n = 200$ (middle row), $n = 500$ (bottom row) samples.

	G_1	G_2	G_3	G_4	G_5	G_6	G_7	G_8	G_9	G_{10}
$ V $	623	493	418	387	169	108	105	87	74	14
PC	99%	99%	101%	95%	98%	110%	96%	114%	84%	85%
FCI	96%	95%	94%	92%	90%	89%	82%	96%	76%	80%
lFCI	94%	94%	92%	91%	89%	87%	80%	91%	73%	81%

Table 1: Average directed Structural Hamming Distances (dSHD) between outputs and truth, as percentage of the glasso baseline.

of genes and infer their causal relations using PC, FCI, and lFCI. In the ℓ -th experiment, we randomly sample half of the genes from V_i as observed nodes, denoted V_i^ℓ , and treat the rest as unobserved. To make the problem scientifically interesting, we assign higher probability of being observed to genes with degree more than 8 in \tilde{G} . The ground truth is the MAG deduced from G_i^T over V_i^ℓ . In practice, we use the MAG deduced from \tilde{G}_i , and call this MAG \tilde{G}_i^ℓ . We run PC, FCI and lFCI (setting $\eta = 2$ and $\gamma = \lceil \log |V_i| \rceil$) with different threshold levels (α); for each output (PAG), we find a MAG compatible with it, compute the likelihood of the corresponding Gaussian graphical model, and compute the eBIC score with tuning parameter set to 0.5; we allow different α levels for PC, FCI and lFCI that each maximizes the eBIC score. For comparison, we also run a baseline method: we first infer an undirected graph using graphical lasso (glasso) (Friedman et al., 2007) with penalty tuned by eBIC. For this baseline, we assign edge marks (arrowhead, tail, and circle) randomly to obtain a mixed graph.

We compare the estimated graphs with \tilde{G}_i^ℓ . More specifically, we compare the graphs estimated using only observed variables V_i^ℓ , to the “truth” deduced from the network over V_i . We use the directed Structural Hamming Distance (dSHD) to measure the difference between the estimated graph and \tilde{G}_i^ℓ . For directed graphs, dSHD is defined as the number of edge additions, deletions or flips to transform one graph into another. In mixed graphs, we count edges with two mismatching marks as a “flip” and edges with one mismatching mark as half a “flip”. We repeat this process 40 times for each V_i , $i = 1, \dots, 10$.

The results in Table 1 demonstrate that, as expected, FCI and lFCI outperforms PC. They also suggest that lFCI slightly outperforms or is comparable with FCI in 9 of the 10 subgraphs. The improvement is more pronounced in large graphs and graphs containing many “hubs” (e.g., component 1, 3 and 5), but is nonetheless persistent in all subgraphs.

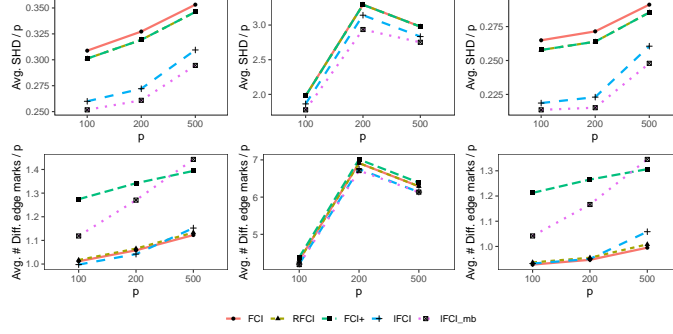


Figure 8: Average Structural Hamming Distances divided by p (top row) and difference in edge marks divided by p (bottom row) with $p = 100, 200, 500$ from Erdős-Rényi (left column), power-law (middle column), and Watts-Strogatz (right column) graphs based on $n = 200$.

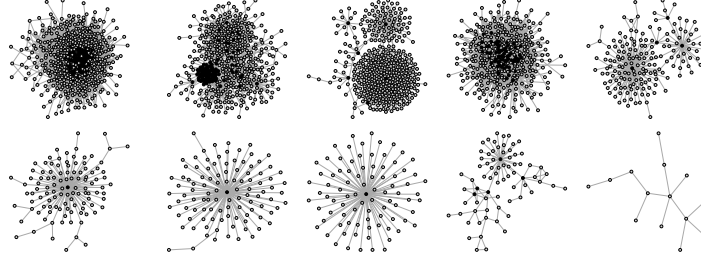


Figure 9: Visualization of the BIOGRID networks G_1^B, \dots, G_{10}^B .

8 Discussion

Causal structure learning from observational data is an important and challenging problem. The challenges are compounded in the presence of unmeasured confounding and selection bias. The gold-standard approach for this task, the FCI algorithm (Spirtes et al., 2000), and its relatives, RFCI (Colombo et al., 2012) and FCI+ (Claassen et al., 2013), are based on neighborhood-based search strategies that become inefficient in graphs with unbounded maximum degrees. However, such graphs are abundant in biological and physical systems. To facilitate causal structure discovery in such settings, our local FCI (IFCI) algorithm utilizes the *local separation property* of large (random) networks (Anandkumar et al., 2012a) by considering an alternative local-graph-based search strategy focused on short paths between pairs of observed nodes. This idea applies naturally to linear Gaussian structural equation models (SEMs), in which conditional independence is equivalent to zero partial correlation. However, the proposed algorithm only relies on conditional independence tests, and can be, in principle, applied to a wider collection of models in which causal relations are well-characterized by local structures. Extending this idea to more general distributions, using, e.g., Gaussian copulas (Harris and Drton, 2013), or using conditional mutual information (Anandkumar et al., 2012b) can be fruitful directions of future research.

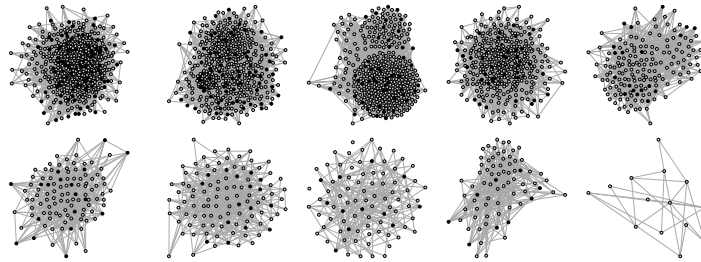


Figure 10: Visualization of the estimated TCGA networks $\tilde{G}_1, \dots, \tilde{G}_{10}$.

For linear Gaussian SEMs, Assumption 5 gives a condition under which IFCI consistently learns a correct PAG. The conditional covariances involved in this assumption can be expressed as summations over products along *treks*, which are particular paths in the graph (Sullivant et al., 2010; Draisma et al., 2013); see also the discussion in Section 3 of the Supplementary Material. From this point of view, conditioning on the local separators proposed in Section 3 can be regarded as eliminating the contribution of short treks. It is then intuitive that the remaining long treks, each of which gives a product of many correlations, only make lower-order contributions. However, we found it difficult to formalize this argument into an assumption that weakens Assumption 6 as this would require explicitly controlling the number of long treks and their overall contribution to conditional covariances.

References

- Ali, R. A., Richardson, T. S., and Spirtes, P. (2009). Markov equivalence for ancestral graphs. *Ann. Statist.*, 37(5B):2808–2837.
- Anandkumar, A., Hassidim, A., and Kelner, J. (2011). Topology discovery of sparse random graphs with few participants. *SIGMETRICS Perform. Eval. Rev.*, 39(1):253–264.
- Anandkumar, A., Tan, V. Y. F., Huang, F., and Willsky, A. S. (2012a). High-dimensional Gaussian graphical model selection: walk summability and local separation criterion. *J. Mach. Learn. Res.*, 13:2293–2337.
- Anandkumar, A., Tan, V. Y. F., Huang, F., and Willsky, A. S. (2012b). High-dimensional structure estimation in Ising models: local separation criterion. *Ann. Statist.*, 40(3):1346–1375.
- Bollobás, B. and Béla, B. (2001). *Random Graphs*. Cambridge Studies in Advanced Mathematics. Cambridge University Press.
- Cancer-Genome-Atlas-Research-Network (2012). Comprehensive genomic characterization of squamous cell lung cancers. *Nature*, 489(7417):519–525.
- Chen, H. and Sharp, B. M. (2004). Content-rich biological network constructed by mining pubmed abstracts. *BMC Bioinformatics*, 5:147 – 147.
- Chung, F. and Lu, L. (2006). *Complex Graphs and Networks (CBMS Regional Conference Series in Mathematics)*. American Mathematical Society.
- Claassen, T., Mooij, J. M., and Heskes, T. (2013). Learning sparse causal models is not NP-hard. In *Proceedings of the 29th Conference on Uncertainty in Artificial Intelligence*.
- Colombo, D. and Maathuis, M. H. (2014). Order-independent constraint-based causal structure learning. *J. Mach. Learn. Res.*, 15:3741–3782.
- Colombo, D., Maathuis, M. H., Kalisch, M., and Richardson, T. S. (2012). Learning high-dimensional directed acyclic graphs with latent and selection variables. *Ann. Statist.*, 40(1):294–321.
- Dembo, A. and Montanari, A. (2010). Ising models on locally tree-like graphs. *Ann. Appl. Probab.*, 20(2):565–592.
- Dommers, S., Giardinà, C., and van der Hofstad, R. (2010). Ising models on power-law random graphs. *J. Stat. Phys.*, 141(4):638–660.
- Draisma, J., Sullivant, S., and Talaska, K. (2013). Positivity for Gaussian graphical models. *Adv. in Appl. Math.*, 50(5):661–674.
- Drton, M. and Richardson, T. S. (2008). Binary models for marginal independence. *J. R. Stat. Soc. Ser. B Stat. Methodol.*, 70(2):287–309.
- Foygel, R. and Drton, M. (2010). Extended Bayesian information criteria for Gaussian graphical models. In *Advances in Neural Information Processing Systems 23*, pages 604–612.
- Friedman, J., Hastie, T., and Tibshirani, R. (2007). Sparse inverse covariance estimation with the graphical lasso. *Biostatistics*, 9(3):432–441.
- Harris, N. and Drton, M. (2013). PC algorithm for nonparanormal graphical models. *J. Mach. Learn. Res.*, 14(1):3365–3383.

- Ideker, T. and Krogan, N. J. (2012). Differential network biology. *Molecular Systems Biology*, 8(1):565.
- Kalisch, M. and Bühlmann, P. (2007). Estimating high-dimensional directed acyclic graphs with the PC-algorithm. *J. Mach. Learn. Res.*, 8:613–636.
- Kalisch, M., Mächler, M., Colombo, D., Maathuis, M. H., and Bühlmann, P. (2012). Causal inference using graphical models with the R package pcalg. *Journal of Statistical Software*, 47(11):1–26.
- Kleinberg, J. M., Kumar, R., Raghavan, P., Rajagopalan, S., and Tomkins, A. S. (1999). The web as a graph: Measurements, models, and methods. In *Proceedings of the 5th Annual International Conference on Computing and Combinatorics*, pages 1–17.
- Lin, L., Drton, M., and Shojaie, A. (2016). Estimation of high-dimensional graphical models using regularized score matching. *Electron. J. Statist.*, 10(1):806–854.
- Liu, W. and Luo, X. (2015). Fast and adaptive sparse precision matrix estimation in high dimensions. *J. Multivariate Anal.*, 135:153–162.
- Maathuis, M., Drton, M., Lauritzen, S., and Wainwright, M., editors (2019). *Handbook of graphical models*. CRC Press, Boca Raton, FL.
- Malioutov, D. V., Johnson, J. K., and Willsky, A. S. (2006). Walk-sums and belief propagation in Gaussian graphical models. *J. Mach. Learn. Res.*, 7:2031–2064.
- McKay, B. D., Wormald, N. C., and Wysocka, B. (2004). Short cycles in random regular graphs. *Electron. J. Combin.*, 11(1):Research Paper 66, 12.
- Molloy, M. and Reed, B. (1995). A critical point for random graphs with a given degree sequence. *Random Structures Algorithms*, 6(2-3):161–179.
- Ogarrio, J. M., Spirtes, P., and Ramsey, J. (2016). A hybrid causal search algorithm for latent variable models. In *Proceedings of the 8th International Conference on Probabilistic Graphical Models*, pages 368–379.
- Ravikumar, P., Wainwright, M. J., Raskutti, G., and Yu, B. (2011). High-dimensional covariance estimation by minimizing ℓ_1 -penalized log-determinant divergence. *Electron. J. Stat.*, 5:935–980.
- Richardson, T. and Spirtes, P. (2002). Ancestral graph Markov models. *Ann. Statist.*, 30(4):962–1030.
- Shojaie, A. (2021). Differential network analysis: a statistical perspective. *Wiley Interdiscip. Rev. Comput. Stat.*, 13(2):e1508, 16.
- Sondhi, A. and Shojaie, A. (2019). The reduced PC-algorithm: improved causal structure learning in large random networks. *J. Mach. Learn. Res.*, 20:Paper No. 164, 31.
- Spirtes, P. (2001). An anytime algorithm for causal inference. In *Proceedings of the 8th International Workshop on Artificial Intelligence and Statistics*, volume R3, pages 278–285.
- Spirtes, P., Glymour, C., and Scheines, R. (2000). *Causation, Prediction, and Search, Second Edition*. MIT Press: Cambridge.
- Stark, C. (2006). BioGRID: a general repository for interaction datasets. *Nucleic Acids Research*, 34(90001):D535–D539.
- Sullivant, S., Talaska, K., and Draisma, J. (2010). Trek separation for Gaussian graphical models. *Ann. Statist.*, 38(3):1665–1685.
- Tsamardinos, I., Brown, L. E., and Aliferis, C. F. (2006). The max-min hill-climbing Bayesian network structure learning algorithm. *Mach. Learn.*, 65(1):31–78.
- van der Zander, B. and Liskiewicz, M. (2019). Finding minimal d-separators in linear time and applications. In *Proceedings of the 35th Conference on Uncertainty in Artificial Intelligence*.
- Watts, D. J. and Strogatz, S. H. (1998). Collective dynamics of ‘small-world’ networks. *Nature*, 393(6684):440–442.
- Yu, S., Drton, M., and Shojaie, A. (2019). Generalized score matching for non-negative data. *J. Mach. Learn. Res.*, 20:Paper No. 76, 70.
- Zhang, J. (2008). On the completeness of orientation rules for causal discovery in the presence of latent confounders and selection bias. *Artif. Intell.*, 172(16-17):1873–1896.

A Proofs

Proof of Lemma 3. We prove the case of $\eta = 3$ by enumerating all possible configurations of $G_\gamma(i, j)$ in the extended neighborhood of i and constructing a small m -separator for each one. Since G is a MAG, i and j cannot be ancestors of each other. Without loss of generality, we suppose $i \notin \text{an}(G, j)$. We use the following three facts.

1. Let $D_{G_\gamma(i, j)}(u, v)$ be the shortest path distance in the local graph, and let $N_k = \{v \in V_\gamma(i, j) : D_{G_\gamma(i, j)}(v, i) = k\}$ for each $k = 1, 2, \dots, \gamma$. Then for each $k \leq \gamma$, there are at most η paths from i to N_k . Hence, $|\text{ne}(G_\gamma(i, j), u)| \leq \eta$.
2. Consider the two set of edges $e_k^b = \{(u, v) : u \in \text{adj}(G_\gamma(i, j), v), u \in N_k, v \in N_{k+1}\}$ and $e_k^m = \{(u, v) : u \in \text{adj}(G_\gamma(i, j), v), u, v \in N_k\}$. For each $k \leq \gamma$, every node in N_k has at least one edge in e_k^b or e_k^m (it cannot be a “deadend”), and $|e_k^b| + |e_k^m| \leq \eta$.
3. In the MAG G , if (u, v) are non-adjacent, then there is no inducing path between them, i.e., no path on which every node is a collider and ancestor of u or v .

The details are given in the Supplementary Material. \square

Proof of Lemma 5. By Lemma 1, it suffices to consider two nodes i and j that are non-adjacent in G and show that $V_\gamma(i, j) \setminus \{i, j\} \subseteq J_\gamma(i, j, C)$. By definition, any $v \in V_\gamma(i, j) \setminus \{i, j\}$ lies on a short path between i, j , so $D_G(i, v) + D_G(j, v) \leq \gamma$. Since i, j are not adjacent, we know $C = C_{-ij}$ is a supergraph of G . Hence, $D_{C_{-ij}}(i, v) \leq D_G(i, v)$ and $D_{C_{-ij}}(j, v) \leq D_G(j, v)$, which implies $D_{C_{-ij}}(i, v) + D_{C_{-ij}}(j, v) \leq \gamma$, and $v \in V_\gamma(i, j) \setminus \{i, j\} \subseteq J_\gamma(i, j, C)$. \square

To prove Theorem 2, we first show an error bound for sample partial correlations.

Lemma 8. Assume $W = (W_1, \dots, W_p)$ is a zero-mean random vector with covariance matrix Σ such that each $W_i/\Sigma_{ii}^{1/2}$ is sub-Gaussian with parameter σ . Assume σ is bounded, and the minimal eigenvalue of all $(\eta + 2) \times (\eta + 2)$ submatrices of Σ are bounded below by $\lambda_{\min} > 0$. If for $\zeta > 0$ and $\epsilon > 0$ satisfying $\epsilon < 16(\eta + 2)\lambda_{\min}^{-2} \max_i(\Sigma_{ii})(1 + 4\sigma^2)$ we have

$$n \geq \{\log(p^2 + p) - \log(2\zeta)\} 128(1 + 4\sigma^2)^2 \max_i(\Sigma_{ii})^2 (\eta + 2)^2 (\lambda_{\min}^{-1} + \lambda_{\min}^{-2} (1 + 2/\epsilon))^2, \quad (4)$$

then the empirical partial correlation obtained from n samples satisfies

$$\mathbb{P} \left\{ \max_{i \neq j, |S| \leq \eta} |\rho(i, j|S) - \widehat{\rho}(i, j|S)| \geq \epsilon \right\} \leq \zeta. \quad (5)$$

Proof. Set $\delta = \epsilon \lambda_{\min}^2 / [(\epsilon + \epsilon \lambda_{\min} + 2)(\eta + 2)]$. Our choice of δ satisfies $\delta \in (0, 8 \max_i(\Sigma_{ii})(1 + 4\sigma^2))$. Then by Lemma 1 in Ravikumar et al. (2011), we obtain the following inequality,

$$\mathbb{P} \left(|\widehat{\Sigma}_n(i, j) - \Sigma(i, j)| > \delta \right) \leq 4 \exp \left\{ - \frac{n\delta^2}{128(1 + 4\sigma^2)^2 \max_i(\Sigma_{ii})^2} \right\}$$

With the stated n , we have $\mathbb{P} \left(|\widehat{\Sigma}_n(i, j) - \Sigma(i, j)| > \delta \right) \leq 2\zeta/(p^2 + p)$. A union bound over all the entries yields $\mathbb{P} \left(\|\widehat{\Sigma}_n - \Sigma\|_\infty > \delta \right) \leq \zeta$. By Lemma 4 of Harris and Drton (2013), for all i, j and $|S| \leq \eta$, $\|\widehat{\Sigma}_n - \Sigma\|_\infty \leq \delta$ implies $|\rho(i, j|S) - \widehat{\rho}(i, j|S)| < \epsilon$. Therefore (5) holds. \square

Proof of Theorem 2. By Lemma 6, if all condition independence tests for conditioning set $|S| \leq \eta$ make correct decisions, then the output of IFCI is sound, and under Assumption 1 the output is complete. We aim to show that this is true on a high probability event.

First suppose we make conditional independence decisions by rejecting the null if only if $|\widehat{\rho}(i, j|S)| > \lambda/2$, where λ is from Assumption 4. Define the following event,

$$A = \left[\max_{i \neq j, |S| \leq \eta} |\rho(i, j|S) - \widehat{\rho}(i, j|S)| \leq \lambda/2 \right].$$

By Lemma 8, for any $\zeta > 0$, with $n = \Omega((\log p)^{1/(1-2\zeta)})$ we have $\mathbb{P}\{A\} > 1 - \zeta$. Given A , it holds that for all i, j and $|S| \leq \eta$, $|\widehat{\rho}(i, j|S)| > \lambda/2$ if and only if $|\rho(i, j|S)| > \lambda$. Therefore, with high probability, all the conditional independence decisions are correct and the output is sound. The completeness result follows Lemma 6.

Next, suppose we make conditional independence decisions by comparing z -transformed partial correlations to normal quantiles. It is shown in Appendix A of Harris and Drton (2013) that this approach is equivalent to the thresholding rule with the following significance levels,

$$\alpha_n = 2 \left(1 - \Phi \left(0.5\sqrt{n-3} \log \left(\frac{1 + \lambda/3}{1 - \lambda/3} \right) \right) \right).$$

\square

	p	ER				PL				WS			
		FCI	FCI+	IFCI	IFCImb	FCI	FCI+	IFCI	IFCImb	FCI	FCI+	IFCI	IFCImb
%Recovered	20	1	1	1	1	1	1	1	1	1	1	1	1
	50	1	1	1	1	1	1	1	1	1	1	1	1
	100	1	1	1	1	1	1	1	1	1	1	1	1
ρ^*	20	0	0	0	0	0	0	0	0	0	0	0	0
	50	0	0	0	0	0	0	0	0	0	0	0	0
	100	0	0	0.004	0	0	0	0.009	0	0	0	0.001	0
$\log(\#CI)$	20	8.3	6.7	6.3	5.7	10.9	9.3	6.2	5.7	6.6	6.1	5.8	5.3
	50	10.4	8.1	8.2	7.4	17.1	13.1	7.7	7.0	8.5	7.7	7.6	6.9
	100	11.9	8.9	8.9	8.2	15.2	12.1	8.9	8.2	9.8	8.8	8.9	8.2
m_{reach}	20	4.9	4.0	2.9	1.6	8.7	7.9	2.4	1.3	4	3	3	1
	50	6.2	5.2	3.2	2.0	13.6	12.5	2.8	1.4	5	4	3	2
	100	6.9	6.0	3.2	1.8	12.7	12.7	2.7	1.3	6	5	3	2

Table 2: Average performance of population version of FCI, FCI+, IFCI and IFCImb with graphs of size $p \in \{20, 50, 100\}$ and fixed $\gamma = 6$.

Proof of Corollary 1. Under the assumptions, there are always small neighborhood-based separators between non-adjacent nodes (see the proof for Lemma 2), and therefore the approximate-rPC, like rPC, consistently recovers correct skeletons. The orientation step is also sound and complete (See proof of Lemma 6 for $\mathcal{R}_0 - \mathcal{R}_3$.) \square

We next show theoretical guarantees for Algorithm 2 with estimated Markov blanket.

Theorem 3. *Under Assumptions 2, 4, 3, 5, and suppose $n = \Omega((\log p)^{1/(1-2c)})$. Suppose γ is large enough such that $\text{mb}_\gamma(G, v) = \text{mb}(G, v)$ for all $v \in V$. Suppose there exists a sequence $\tau_{n,p} \rightarrow 0$ such that the estimated precision matrix satisfies $\|\hat{\Theta} - \Theta\|_\infty \leq \tau_{n,p}$ with high probability. Also assume $\min_{i \in \text{adj}(G, j)} |\Theta_{ij}| \geq 2\tau_{n,p}$. Then there exists a sequence $\alpha_n \rightarrow 0$ such that Algorithm 2 consistently learns a PAG for $[G]$. Moreover, if Assumption 1 holds, then it consistently learns the maximally informative PAG.*

Remark 1. To estimate the precision matrix, we can use in particular generalized score matching (Lin et al., 2016; Yu et al., 2019) or equivalently the SCIO algorithm (Liu and Luo, 2015), which satisfies $\|\hat{\Theta} - \Theta\|_\infty = O_p\left(\sqrt{s_p \log(p)/n}\right)$, where $s_p = \max_{i \in V} |\text{mb}_\gamma(G, i)|$.

Proof of Theorem 3. Under stated assumptions on precision and beta-min, with high probability, $\{(i, j) : i \in \text{adj}(G, j)\} \subseteq \{(i, j) : (i, j) \in \text{supp}(\hat{\Theta})\} \subseteq \{(i, j) : i \in \text{mb}_\gamma(G, j)\}$. The rest of this proof is identical to Theorem 2, with η replaced by $\eta - 1$, following Lemma 4. \square

B Simulations with local-graph separation oracle

In this section we investigate the performance of population version of FCI, FCI+ and IFCI. We use the exact same settings as the simulation study in Section 6. We run FCI and FCI+ with oracle m -separations, and IFCI with oracle γ -local-separations, with $\gamma = 6$. The experiment is repeated 50 times. In the power-law setting with $p = 100$, FCI is usually much more computationally burdensome than FCI+ and IFCI. Due to this limitation, we only report the runs in which FCI terminated within 8 hours. Results are shown in Table 2.

Performances of the methods are evaluated by the proportion of cases in which the true (unique) maximally informative PAG is recovered. Computational costs are compared based on the total number of CI tests and the maximal reach levels. We also check Assumption 5 directly with $\rho^* = \max_{(i,j) \notin E} \min_{S \in \mathcal{S}_{\eta,\gamma}(i,j)} |\rho(i, j|S)|$ and report the median over all cases. Note that FCI/FCI+ are exact algorithms, meaning they recover the maximally informative PAG in all cases, because m -separations always correspond to zero partial correlations. IFCI/IFCImb are not guaranteed to be complete if Assumption 5 is violated — though their outputs are correct PAGs, they are sometimes not maximally informative. The proposed methods show improvement on the computational aspects: the number of tests are consistent over different graph generating schemes, whereas FCI/FCI+ could suffer in power-law cases. The maximum reach level (m_{reach}) confirms the results in Section 3 — in most cases the local separators are indeed as small as 3.

Supplementary Material for *Causal Structural Learning Via Local Graphs**

Wenyu Chen¹, Mathias Drton², and Ali Shojaie³

¹Department of Statistics, University of Washington, Seattle, WA, USA

²Department of Mathematics, Technical University of Munich, München, Germany

³ Department of Biostatistics, University of Washington, Seattle, WA, USA

January 2, 2022

1 Additional results

Definition 1 (PAG). Let $G = (X \cup L \cup Z, E)$ be a DAG, and H be a simple graph with vertex set X and edges of the type \rightarrow , \Rightarrow , \Leftarrow , $\Leftarrow\Leftarrow$, \leftrightarrow , $-$, or $\circ-$. Then H is a PAG representing G if and only if the following four conditions hold:

1. The absence of an edge between two vertices i and j in H implies that there exists a subset $Y \subseteq X \setminus \{i, j\}$ such that i and j are m -separated given $(Y \cup Z)$.
2. The presence of an edge between two vertices i and j in H implies that i and j are m -connected given $(Y \cup Z)$ for all subsets $Y \subseteq X \setminus \{i, j\}$.
3. If an edge between i and j in H has an arrowhead at j , then $j \notin \text{an}(G, i \cup Z)$.
4. If an edge between i and j in H has a tail at j , then $j \in \text{an}(G, i \cup Z)$.

2 Additional Proofs

Proof of Lemma 3. 1. $|\text{ne}(G_\gamma(i, j), i)| = 1$. (Figure 1) Denote the only neighbor as u . If $i \rightarrow u$ or $i \leftrightarrow u$ but $u \notin \text{an}(G_\gamma(i, j), j)$, then $S_\gamma(i, j) = \emptyset$. If $i \leftarrow u$ or $i - u$, then $S_\gamma(i, j) = \{u\}$. If $i \leftrightarrow u$ and $u \in \text{an}(G_\gamma(i, j), j)$, then there must be an edge $u \rightarrow w$ and $w \in \text{an}(G_\gamma(i, j), j)$. If $\text{ne}(G_\gamma(i, j), u) = \{i, w\}$ then $S_\gamma(i, j) = \{u\}$. Now discuss cases with additional neighbors.

- (a) If $\text{ne}(G_\gamma(i, j), u) = \{i, w, v\}$, we have $S_\gamma(i, j) = \{u\}$ if $u \rightarrow v$ or $u \leftrightarrow v$ but $v \notin \text{an}(G_\gamma(i, j), j)$; also $S_\gamma(i, j) = \{u, v\}$ if $u \leftarrow v$ or $u \leftrightarrow v$ and $v \in \text{an}(G_\gamma(i, j), j)$ and v has exactly one neighbor other than u (it is allowed to be w). If v has 2 neighbors other than u , and neither is child of v , then $v \notin \text{an}(G_\gamma(i, j), j)$, which is covered in the previous case. Now suppose $v \rightarrow x$ and there is also an edge $v \star\star y$, in which case $|e_2^b| + |e_2^m| = 3$. We have $S_\gamma(i, j) = \{u, v, y\}$ if $v \leftarrow y$ or $v \leftrightarrow y$ and $y \in \text{an}(G_\gamma(i, j), j)$, and otherwise $S_\gamma(i, j) = \{u, v\}$.
- (b) If $\text{ne}(G_\gamma(i, j), u) = \{i, w, v, x\}$, then $|e_2^b| = 3$ and $S_\gamma(i, j) \subseteq \{u, v, x\}$.
2. $|\text{ne}(G_\gamma(i, j), i)| = 2$. Denote the neighbors as u and v . We discuss the direction of the two edges $i \star\star u$ and $i \star\star v$. If the directions are $(\rightarrow, \rightarrow)$, then $S_\gamma(i, j) = \emptyset$. If $(\leftarrow, \rightarrow)$, then $S_\gamma(i, j) = \{u\}$. If (\leftarrow, \leftarrow) or $(-, \leftarrow)$ or $(-, -)$, then $S_\gamma(i, j) = \{u, v\}$.
 - (a) If $(\leftrightarrow, \leftarrow)$, then we need to discuss neighbors of u , too. If $u \in \text{adj}(G_\gamma(i, j), v)$, then $u \star\star v$ is a merging edge, and by Fact 2, u and v have in total no more than 2 bearing edges of order 2. If u is not ancestral to i or j , then $S_\gamma(i, j) = \{v\}$. The case of $u \notin \text{an}(G_\gamma(i, j), \{i, j\})$ is trivial. If

*This work has received funding from the U.S. National Institutes of Science (NSF) and of Health (NIH) under grants DMS-1161565, DMS-1561814, and R01GM114029, and from the European Research Council (ERC) under the European Union's Horizon 2020 research and innovation programme (grant agreement No 883818).

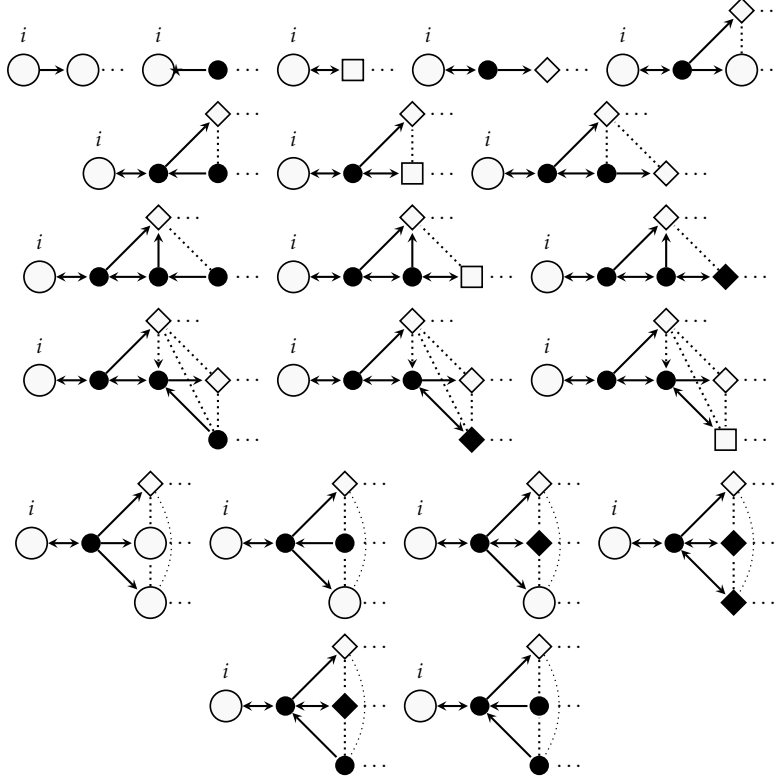


Figure 1: Local graph configurations with $\eta = 3$ and $|\text{ne}(G_\gamma(i, j), i)| = 1$. A separator (not necessarily minimal) is marked with shade. Marked edge represents the pattern of $G_\gamma(i, j)$, while absence of an edge represents the absence pattern of $G_\gamma(i, j)$. Ellipses between nodes means this edge is allowed to occur in $G_\gamma(i, j)$, as long as it agrees with the MAG property and local-path property. The square shape represents a node with no outgoing edge (except the marked ones). The diamond shape represents a node that controls whether the separator is minimum — if this node is not ancestor of j , then smaller separator exists.

$u \in \text{an}(G_\gamma(i, j), \{i, j\})$, then u has at least one outgoing edge. If the outgoing edge is $u \rightarrow v$ (second row of Figure 2), there are two sub-cases. If v has an bearing edge of order 2, then u has only one other neighbor, call it x , and we condition on x if and only if $u \leftarrow x$ or $u \leftrightarrow x$ and $x \in \text{an}(G_\gamma(i, j), j)$. If v has no bearing edge, then u can have at most 2 other neighbors. However, these bearing edges must not have arrow at u , due to the inducing path interpretation of MAG. Therefore we do not need to condition on these additional neighbors.

If the outgoing edge is not $u \rightarrow v$ (third row of Figure 2), then there is some edge $u \rightarrow w$. If v has an bearing edge of order 2, then u no other neighbor than $\{i, u, w\}$. If v has no bearing edge, then u could have one additional neighbor, call it x , and we condition on x if and only if $u \leftarrow x$ or $u \leftrightarrow x$ and $x \in \text{an}(G_\gamma(i, j), j)$.

If $u \notin \text{adj}(G_\gamma(i, j), v)$ (fourth row of Figure 2), then u has at most two additional neighbors. If none of them are child of u , then $u \notin \text{an}(G_\gamma(i, j), \{i, j\})$ and $S_\gamma(i, j) = \{v\}$; If $u \rightarrow w$, $u \star \star x$ then we condition on x if and only if $u \leftarrow x$ or $u \leftrightarrow x$ and $x \in \text{an}(G_\gamma(i, j), j)$.

- (b) if $(\leftrightarrow, \rightarrow)$, the situations are simpler since we never condition on v . Since v must have either a bearing edge or a merging edge, u can have at most 2 bearing edges. If $u \in \text{an}(G_\gamma(i, j), j)$, then one of the edges is $u \rightarrow w$. As for the other one, $u \star \star x$, we condition on x if and only if $u \leftarrow x$ or $u \leftrightarrow x$ and $x \in \text{an}(G_\gamma(i, j), j)$.
- (c) If $(\leftrightarrow, \leftrightarrow)$: If neither of u and v are ancestral to j , then $S_\gamma(i, j) = \emptyset$. If both are ancestral to j (row 2-3 and first 2 figures of row 4 in Figure 3),

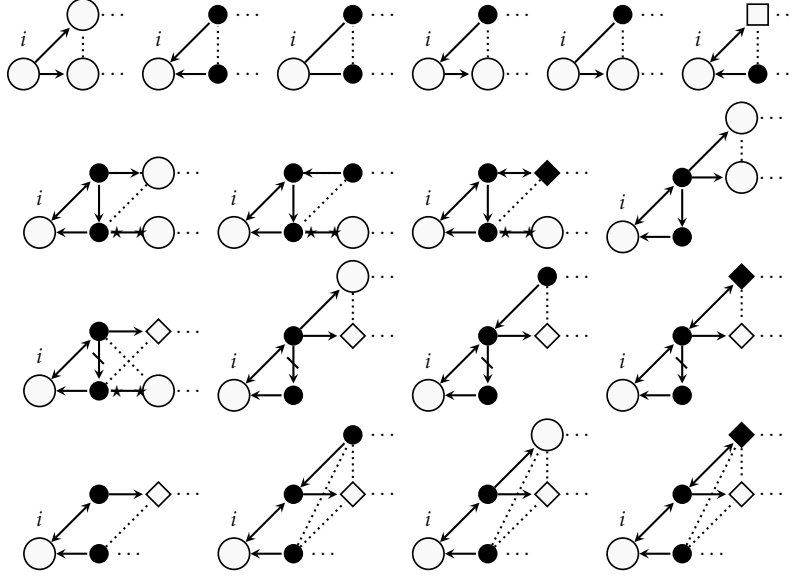


Figure 2: Local graph configurations with $\eta = 3$ and $|\text{ne}(G_\gamma(i, j), i)| = 2$. (continues in Figure 3). A separator (not necessarily minimal) is marked with shade. Marked edge represents the pattern of $G_\gamma(i, j)$, while absence of an edge represents the absence pattern of $G_\gamma(i, j)$. Ellipses between nodes means this edge is allowed to occur in $G_\gamma(i, j)$, as long as it agrees with the MAG property and local-path property. The square shape represents a node with no outgoing edge (except the marked ones). The diamond shape represents a node that controls whether the separator is minimum — if this node is not ancestor of j , then smaller separator exists.

then they each has a outgoing edge. Then by Fact 2, there is at most one other bearing edge. WLOG, suppose u has $u \rightarrow w$ and $u \star \star x$. Then $S_\gamma(i, j) = \{u, v, x\}$ if $x \in \text{an}(G_\gamma(i, j), \{u, j\})$ and otherwise $S_\gamma(i, j) = \{u, v\}$. If u is ancestral to j and v is not, then still u has one outgoing edge and at most one other edge. Then $S_\gamma(i, j) = \{u, x\}$ if $x \in \text{an}(G_\gamma(i, j), \{u, j\})$ and otherwise $S_\gamma(i, j) = \{u\}$.

3. $|\text{ne}(G_\gamma(i, j), i)| = 3$. Denote the three neighbors of i as u, v, w . By Fact 2, they each has at most one bearing edge. Therefore we do not need to look further, and $S_\gamma(i, j) \subseteq \{u, v, w\}$.

□

The following proof is similar to Lemma 2 of Sondhi and Shojaie (2019) with slight modification, we show the proof here for completeness.

Proof of Lemma 5.7. We write

$$\begin{aligned} \Sigma &= (I - B)^{-1} \Omega (I - B)^{-\top} \\ &= \left(\sum_{r=0}^{p-1} B^r \right) \Omega \left(\sum_{r=0}^{p-1} B^r \right)^\top \\ &= \left(\sum_{r=0}^{\gamma} B^r + \sum_{r=\gamma+1}^{p-1} B^r \right) \Omega \left(\sum_{r=0}^{\gamma} B^r + \sum_{r=\gamma+1}^{p-1} B^r \right)^\top \end{aligned}$$

Denote $\Lambda_H = \sum_{r=0}^{\gamma} B^r$ and $R_\gamma = \sum_{r=\gamma+1}^{\infty} B^r = \sum_{r=\gamma+1}^{p-1} B^r$. By the directed β -summability assumption, we have $\|\Lambda_H\| \leq \frac{1-\beta^{\gamma+1}}{1-\beta}$ and $\|R_\gamma\| \leq \frac{\beta^{\gamma+1}-\beta^p}{1-\beta}$. Now we can bound the difference between Σ and the local approximation version $\Sigma_H := \Lambda_H \Omega \Lambda_H^\top$, which only contains paths

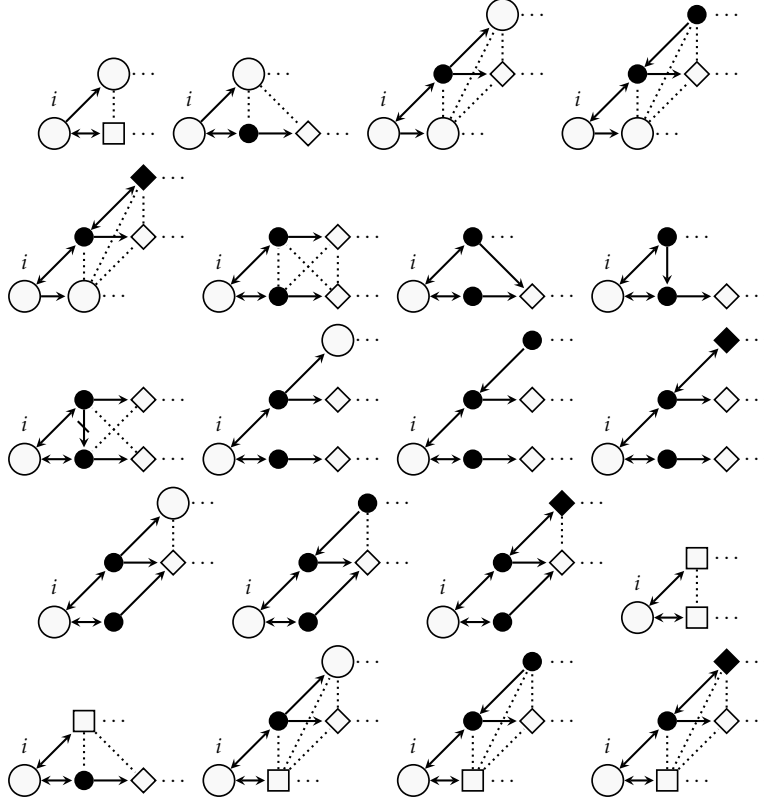


Figure 3: Local graph configurations with $\eta = 3$ and $|\text{ne}(G_\gamma(i, j), i)| = 2$. A separator (not necessarily minimal) is marked with shade. Marked edge represents the pattern of $G_\gamma(i, j)$, while absence of an edge represents the absence pattern of $G_\gamma(i, j)$. Ellipses between nodes means this edge is allowed to occur in $G_\gamma(i, j)$, as long as it agrees with the MAG property and local-path property. The square shape represents a node with no outgoing edge (except the marked ones). The diamond shape represents a node that controls whether the separator is minimum — if this node is not ancestor of j , then smaller separator exists.

no longer than γ .

$$\begin{aligned}
\|\Sigma - \Sigma_H\| &= \|\Lambda_H \Omega R_\gamma^\top + R_\gamma \Omega \Lambda_H^\top + R_\gamma \Omega R_\gamma^\top\| \\
&\leq \|\Omega\| (2\|\Lambda_H\| \|R_\gamma\| + \|R_\gamma\|^2) \\
&\leq \|\Omega\| \left(2 \frac{(1 - \beta^{\gamma+1})\beta^{\gamma+1}}{(1 - \beta)^2} + \frac{\beta^{2\gamma+2}}{(1 - \beta)^2} \right) \\
&= \|\Omega\| \frac{\beta^{\gamma+1}(2 - \beta^{\gamma+1})}{(1 - \beta)^2}
\end{aligned}$$

We write $\gamma^* = \log(\beta)^{-1} (\log M - \log 2 - \log \|\Omega\| - \log(\eta + 2) - \log(1 + 3/\lambda)) - 1$. We invoke the error propagation lemma from Harris and Drton (2013). For any non-adjacent pair (i, j) and a set $S \subseteq V \setminus \{i, j\}$ with $|S| \leq \eta$, whenever $\gamma \geq \gamma^*$, it holds that

$$|\rho(i, j|S) - \rho_H(i, j|S)| \leq \lambda$$

where ρ_H is the partial correlation obtained from Σ_H . Since Σ_H only composes of short paths, $\rho_H(i, j|S_\gamma) = 0$ for every local-graph separator S_γ . Therefore $|\rho(i, j|S_\gamma)| < \lambda$. \square

3 Treks

In this section we provide an algebraic explanation of Assumption 5. In particular, we review the trek representation of partial correlation in linear SEM. The representation clarifies that conditional dependence in a linear SEM is tied to existence of paths/treks in the graph

underlying the model. This allows us to argue that conditional dependence is typically induced by short versus long treks, which in turn provides the basis for exploiting small local separators in our algorithms.

To simplify the discussion, we present the following results assuming there is no selection variables in the graph. Let G be a mixed graph without undirected edges. We define a *trek* from node i to j as a tuple $\tau = (P_L, P_M, P_R)$, where P_L is a directed path from some node s to i , and P_R is a directed path from some node t to j , and P_M is either one bidirected edge $s \leftrightarrow t$ or the empty set when $s = t$. We define the *trek monomial* as $m_\tau = \beta^L \omega_{s,t} \beta^R$, where $\beta^L = \prod_{k \rightarrow i \in P_L} \beta_{kl}$ and $\beta^R = \prod_{k \rightarrow j \in P_R} \beta_{kl}$. Moreover, for sets C and D with $|C| = |D| = k$, we define a *trek system* T from C to D as a set of k treks whose initial nodes exhaust C and final nodes exhaust D . With abuse of notation we write T as a tuple of collections of paths (P_L, P_M, P_R) , and define the *trek system monomial* as the product of trek monomials in the system, i.e., $m_T = \prod_{\tau \in T} m_\tau$. Each trek system determines a permutation of the initial and final nodes, which we call the sign of the system. Let $\mathcal{T}(C, D)$ denote the collection of all trek systems from C to D . By the Cauchy–Binet determinant expansion, we have,

$$\det \Sigma(C, D) = \sum_{R, S \subseteq V, |R|=|S|=k} \det((I - B)^{-\top})_{C,R} \det \Omega_{R,S} \det((I - B)^{-1})_{S,D} \quad (1)$$

$$= \sum_{T \in \mathcal{T}(C,D)} \text{sign}(T) m_T. \quad (2)$$

We say a trek system T has *sided intersection* if two paths in P_L , P_R , or P_M have shared nodes. If T is a trek system between C and D with sided intersections, then its weight m_T is cancelled in the summation in (2), (for a proof, see Sullivant et al., 2010). In other words, the summation in (2) only needs to run over trek systems without sided intersections. Consequently, $\det(\Sigma(i \cup S, j \cup S)) = 0$ if and only if every system of treks from $i \cup S$ to $j \cup S$ has a sided intersection. The later condition is also called *t-separation*. For Gaussian SEMs, in which conditional independence is characterized by zero partial correlation, this means $W_i \perp\!\!\!\perp W_j | W_S$ if and only if $\sum_{T \in \mathcal{T}(i \cup S, j \cup S)} \text{sign}(T) m_T = 0$.

We will show next that Assumption 5 can be expressed as a condition on trek weights. Let $G = (V, E)$ be a MAG. For non-adjacent nodes $i, j \in V$, and $S \subseteq V(G_\gamma) \setminus \{i, j\}$, we denote $\mathcal{T}_\gamma(i, j, S)$ as the collection of trek systems from $i \cup S$ to $j \cup S$ in $G_\gamma(i, j)$, and $\mathcal{T}_\gamma^C(i, j, S) := \mathcal{T}(i \cup S, j \cup S) \setminus \mathcal{T}_\gamma^C(i, j, S)$. By our definition, $\mathcal{T}_\gamma^C(i, j, S)$ only contains treks that goes through a node outside $G_\gamma(i, j)$.

Lemma 1. *Let G be a MAG. Under Assumption 3, if there exists $\beta \in (0, 1)$ such that*

$$\max_{i \notin \text{adj}(G, j)} \min_{S_\gamma \in \mathcal{S}_{\eta, \gamma}(i, j)} \left| \sum_{T \in \mathcal{T}_\gamma^C(i, j, S_\gamma)} \text{sign}(T) m_T \right| = O(\beta^\gamma),$$

where $\mathcal{S}_{\eta, \gamma}(i, j)$ is the collection of γ -local-graph separators of size at most η , then Assumption 5 holds.

Proof. By Definition 4, if a set S_γ is a γ -local-separator of (i, j) , then it is a separator of i and j in $G_\gamma(i, j)$, so all trek systems between $i \cup S_\gamma$ and $j \cup S_\gamma$ have sided intersections in $G_\gamma(i, j)$, and hence also in G . Following Draisma et al. (2013), we only need to take summation over trek systems without sided intersection in G . Therefore,

$$\begin{aligned} \sum_{T \in \mathcal{T}(i, j, S_\gamma)} \text{sign}(T) m_T &= \sum_{T \in \mathcal{T}_\gamma(i, j, S_\gamma)} \text{sign}(T) m_T + \sum_{T \in \mathcal{T}_\gamma^C(i, j, S_\gamma)} \text{sign}(T) m_T \\ &= \sum_{T \in \mathcal{T}_\gamma^C(i, j, S_\gamma)} \text{sign}(T) m_T. \end{aligned}$$

Now denote $\Sigma(i, j | S_\gamma)$ as the (i, j) -th entry of the conditional variance matrix given S_γ . We have

$$\rho(i, j | S_\gamma) = \frac{\Sigma(i, j | S_\gamma)}{\sqrt{\Sigma(i, i | S_\gamma) \Sigma(j, j | S_\gamma)}} = \frac{\sum_{T \in \mathcal{T}(i, j, S_\gamma)} \text{sign}(T) m_T}{\det(\Sigma(S_\gamma, S_\gamma))} \frac{1}{\sqrt{\Sigma(i, i | S_\gamma) \Sigma(j, j | S_\gamma)}}.$$

By the fact that $\Sigma(j, j | S_\gamma) \geq \Sigma(j, j | V \setminus \{j\}) = 1/\omega_{jj}$, and $\det(\Sigma(S_\gamma, S_\gamma)) \geq M^{-\eta}$ under Assumption 3, we have $|\rho(i, j | S_\gamma)| = O(\beta^\gamma)$. \square

4 Choice of γ

Recall the simulation study in Section 6. We randomly generate Erdős-Renyi graphs and power-law graphs with $p = |V| = 200$ nodes and average node degree 2. Edge weights

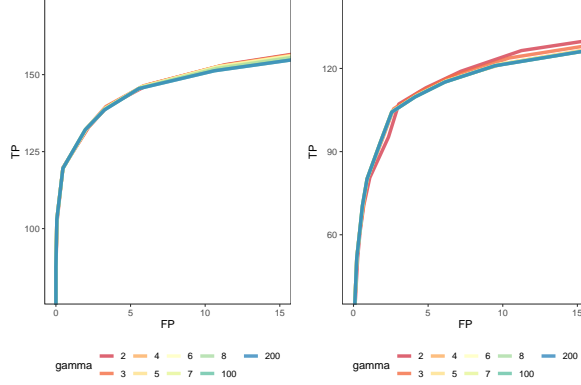


Figure 4: pROC curves of Algorithm 1 with different choices of γ performed on ER graphs (left) and power-law graphs (right).

are drawn uniformly from $\pm[.1, 1]$, and $n = 100$ observations are generated by the `rmvDAG` function. We randomly choose $q = 0.2p$ nodes as latent variables, and the rest as observed. We include no selection variables. We run lFCI with $\gamma = \{2, 3, 4, 5, 6, 7, 8, p/2, p-1\}$, and $\alpha = \{10^{-15}, 10^{-9}, 10^{-8}, 10^{-7}, 10^{-6}, 10^{-3}, 10^{-5}, 10^{-4}, 10^{-3}, 10^{-2}\}$. We repeat the experiment 100 times for each α , and compare the true positive and false positive discoveries of the skeleton of the true PAG.

Figure 4 suggests that as long as γ is large enough, the algorithm yields almost identical outputs. The only exception is the case of power-law graph with $\gamma = 2$, in which the algorithm appears to be too aggressive, and the performance is sub-par on a part of the pROC curve. We also point out that in the “many false positive” part of the curves (i.e., to the right end), methods with smaller γ tends to perform better, since they perform fewer tests. However, that region is only relevant for “discovery”. In general, we recommend using $\gamma = O(\log |V|)$.

5 Simulations with standardized normal coefficients

In this section, we aim to provide evidence that Assumption 5 is satisfied in many common large networks when data is standardized. The fact that in many common scenarios the SEM corresponding to the standardized data has almost all coefficients less than 1 is demonstrated in a simulation study in Appendix B of Sondhi and Shojaie (2019). We further conjecture that the sum of long trek weights are also minimal, by showing the covariance matrix is well approximated using only short treks. For this purpose, we generate a random ER or power-law graph and draw edge weights from either a uniform distribution on $(-10, 10)$ or a normal distribution with mean 0 and standard deviation 3. We intentionally choose wide ranges for the coefficient to allow large fluctuation in the network. Then a SEM in the form of (2) is constructed with this weighted adjacency matrix B and random error variance Ω , where Ω is a diagonal matrix with diagonal entries drawn from a uniform distribution on $(1, 2)$. We denote $\Sigma = (I - B)^{-1}\Omega(I - B)^{-\top}$ and $\tilde{\Sigma}$ as its standardized version, where $\tilde{\Sigma}_{ij} = \Sigma_{ij}/\sqrt{\Sigma_{ii}\Sigma_{jj}}$ for each (i, j) -entry. The standardized data can be seen as drawn from another SEM corresponding to the same graph G , but with different set of parameters $(\tilde{B}, \tilde{\Omega})$, which satisfies $\tilde{\Sigma} = (I - \tilde{B})^{-1}\tilde{\Omega}(I - \tilde{B})^{-\top}$. We compute the maximal entry-wise difference between $\tilde{\Sigma}$ and its short-trek approximation $\tilde{\Sigma}_\gamma = (\sum_{k=0}^{\gamma} \tilde{B}^k)\tilde{\Omega}(\sum_{k=0}^{\gamma} \tilde{B}^k)^{\top}$. We define $d_\gamma := \max_{i,j}(|\tilde{\Sigma} - \tilde{\Sigma}_\gamma|_{i,j})$ and report the smallest γ such that $d_\gamma \leq 10^{-4}$ over 100 iterations. We use the quantity d_γ as a surrogate to check Assumption 5 because we have shown in the proof of Lemma 5.7 that $\|\tilde{\Sigma} - \tilde{\Sigma}_\gamma\| = O(\beta^\gamma)$ is a sufficient condition of Assumption 5.

Figure 5 demonstrates d_γ is indeed very small in most settings with $\gamma \approx \log p$. The results suggest that Assumption 5 is indeed plausible for standardized data.

6 Simulations with local moral graphs

In this section we demonstrate that with large enough γ , the γ -local moral graphs usually coincide with moral graphs. Following the simulation settings in Section 6, in the numerical study below, we generate random DAGs with $p \in \{100, 200, 500\}$ nodes and average node degree 2. Similarly, we also use $\gamma = 5, 6, 7$ for $p = 100, 200, 500$ and randomly choose

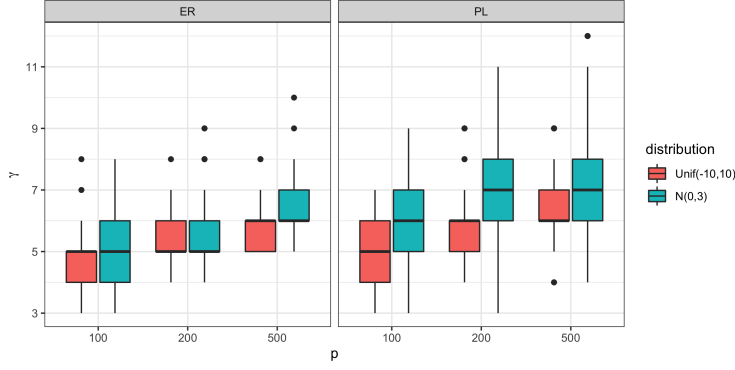


Figure 5: Values of $\min\{\gamma : d_\gamma \leq 10^{-4}\}$ for various settings of ER and power-law graphs, with edge weights drawn from either Uniform $(-10, 10)$ or $N(0, 3^2)$, and $n = 100, 200, 500$. The minimal γ values scale with $\log p$.

	Erdős-Renyi	Power Law	Watts-Strogatz
$p = 100, \gamma = 5$	0.99	1.00	0.96
$p = 200, \gamma = 6$	0.99	1.00	0.97
$p = 500, \gamma = 7$	0.99	1.00	0.97

Table 1: Proportion of random graphs (out of 200 iterations) with γ -local moral graph equal to moral graph.

$q = 0.2p$ nodes as latent nodes, and compute the skeleton of the MAG over the observed ones. We do not introduce selection variables, simply because undirected edges do not contribute to the difference between local and non-local Markov blankets.

We compute the moral graph and γ -local moral graph for each MAG over 200 simulation iterations, and report the proportion of cases when local moral graph is different from the moral graph. The results are reported in Table 1. We see for the choice of γ used in our simulations, almost all local moral graphs are identical to the moral graphs. This is especially likely to be true for power-law graphs, since they tends to have smaller diameter.

7 Search Pools

The graph in Figure 6 is an example in which lFCI may needs to perform more conditional independence tests than FCI.

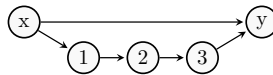


Figure 6: No edge is removed at level 0. At level 1, if the edge (x, y) is checked after removing $(x, 2)$ and $(2, y)$, then FCI performs less CI tests than lFCI (with $\gamma = 5$), because the node 2 is local to x and y but not in their neighborhoods.

References

- Ali, R. A., Richardson, T. S., and Spirtes, P. (2009). Markov equivalence for ancestral graphs. *Ann. Statist.*, 37(5B):2808–2837.
- Anandkumar, A., Hassidim, A., and Kelner, J. (2011). Topology discovery of sparse random graphs with few participants. *SIGMETRICS Perform. Eval. Rev.*, 39(1):253–264.
- Anandkumar, A., Tan, V. Y. F., Huang, F., and Willsky, A. S. (2012a). High-dimensional Gaussian graphical model selection: walk summability and local separation criterion. *J. Mach. Learn. Res.*, 13:2293–2337.
- Anandkumar, A., Tan, V. Y. F., Huang, F., and Willsky, A. S. (2012b). High-dimensional structure estimation in Ising models: local separation criterion. *Ann. Statist.*, 40(3):1346–1375.
- Bollobás, B. and Béla, B. (2001). *Random Graphs*. Cambridge Studies in Advanced Mathematics. Cambridge University Press.
- Cancer-Genome-Atlas-Research-Network (2012). Comprehensive genomic characterization of squamous cell lung cancers. *Nature*, 489(7417):519–525.
- Chen, H. and Sharp, B. M. (2004). Content-rich biological network constructed by mining pubmed abstracts. *BMC Bioinformatics*, 5:147 – 147.
- Chung, F. and Lu, L. (2006). *Complex Graphs and Networks (CBMS Regional Conference Series in Mathematics)*. American Mathematical Society.
- Claassen, T., Mooij, J. M., and Heskes, T. (2013). Learning sparse causal models is not NP-hard. In *Proceedings of the 29th Conference on Uncertainty in Artificial Intelligence*.
- Colombo, D. and Maathuis, M. H. (2014). Order-independent constraint-based causal structure learning. *J. Mach. Learn. Res.*, 15:3741–3782.
- Colombo, D., Maathuis, M. H., Kalisch, M., and Richardson, T. S. (2012). Learning high-dimensional directed acyclic graphs with latent and selection variables. *Ann. Statist.*, 40(1):294–321.
- Dembo, A. and Montanari, A. (2010). Ising models on locally tree-like graphs. *Ann. Appl. Probab.*, 20(2):565–592.
- Dommers, S., Giardinà, C., and van der Hofstad, R. (2010). Ising models on power-law random graphs. *J. Stat. Phys.*, 141(4):638–660.
- Draisma, J., Sullivant, S., and Talaska, K. (2013). Positivity for Gaussian graphical models. *Adv. in Appl. Math.*, 50(5):661–674.
- Drton, M. and Richardson, T. S. (2008). Binary models for marginal independence. *J. R. Stat. Soc. Ser. B Stat. Methodol.*, 70(2):287–309.
- Foygel, R. and Drton, M. (2010). Extended Bayesian information criteria for Gaussian graphical models. In *Advances in Neural Information Processing Systems 23*, pages 604–612.
- Friedman, J., Hastie, T., and Tibshirani, R. (2007). Sparse inverse covariance estimation with the graphical lasso. *Biostatistics*, 9(3):432–441.
- Harris, N. and Drton, M. (2013). PC algorithm for nonparanormal graphical models. *J. Mach. Learn. Res.*, 14(1):3365–3383.
- Ideker, T. and Krogan, N. J. (2012). Differential network biology. *Molecular Systems Biology*, 8(1):565.
- Kalisch, M. and Bühlmann, P. (2007). Estimating high-dimensional directed acyclic graphs with the PC-algorithm. *J. Mach. Learn. Res.*, 8:613–636.
- Kalisch, M., Mächler, M., Colombo, D., Maathuis, M. H., and Bühlmann, P. (2012). Causal inference using graphical models with the R package pcalg. *Journal of Statistical Software*, 47(11):1–26.
- Kleinberg, J. M., Kumar, R., Raghavan, P., Rajagopalan, S., and Tomkins, A. S. (1999). The web as a graph: Measurements, models, and methods. In *Proceedings of the 5th Annual International Conference on Computing and Combinatorics*, pages 1–17.

- Lin, L., Drton, M., and Shojaie, A. (2016). Estimation of high-dimensional graphical models using regularized score matching. *Electron. J. Statist.*, 10(1):806–854.
- Liu, W. and Luo, X. (2015). Fast and adaptive sparse precision matrix estimation in high dimensions. *J. Multivariate Anal.*, 135:153–162.
- Maathuis, M., Drton, M., Lauritzen, S., and Wainwright, M., editors (2019). *Handbook of graphical models*. CRC Press, Boca Raton, FL.
- Malioutov, D. V., Johnson, J. K., and Willsky, A. S. (2006). Walk-sums and belief propagation in Gaussian graphical models. *J. Mach. Learn. Res.*, 7:2031–2064.
- McKay, B. D., Wormald, N. C., and Wysocka, B. (2004). Short cycles in random regular graphs. *Electron. J. Combin.*, 11(1):Research Paper 66, 12.
- Molloy, M. and Reed, B. (1995). A critical point for random graphs with a given degree sequence. *Random Structures Algorithms*, 6(2-3):161–179.
- Ogarrio, J. M., Spirtes, P., and Ramsey, J. (2016). A hybrid causal search algorithm for latent variable models. In *Proceedings of the 8th International Conference on Probabilistic Graphical Models*, pages 368–379.
- Ravikumar, P., Wainwright, M. J., Raskutti, G., and Yu, B. (2011). High-dimensional covariance estimation by minimizing ℓ_1 -penalized log-determinant divergence. *Electron. J. Stat.*, 5:935–980.
- Richardson, T. and Spirtes, P. (2002). Ancestral graph Markov models. *Ann. Statist.*, 30(4):962–1030.
- Shojaie, A. (2021). Differential network analysis: a statistical perspective. *Wiley Interdiscip. Rev. Comput. Stat.*, 13(2):e1508, 16.
- Sondhi, A. and Shojaie, A. (2019). The reduced PC-algorithm: improved causal structure learning in large random networks. *J. Mach. Learn. Res.*, 20:Paper No. 164, 31.
- Spirtes, P. (2001). An anytime algorithm for causal inference. In *Proceedings of the 8th International Workshop on Artificial Intelligence and Statistics*, volume R3, pages 278–285.
- Spirtes, P., Glymour, C., and Scheines, R. (2000). *Causation, Prediction, and Search, Second Edition*. MIT Press: Cambridge.
- Stark, C. (2006). BioGRID: a general repository for interaction datasets. *Nucleic Acids Research*, 34(90001):D535–D539.
- Sullivant, S., Talaska, K., and Draisma, J. (2010). Trek separation for Gaussian graphical models. *Ann. Statist.*, 38(3):1665–1685.
- Tsamardinos, I., Brown, L. E., and Aliferis, C. F. (2006). The max-min hill-climbing Bayesian network structure learning algorithm. *Mach. Learn.*, 65(1):31–78.
- van der Zander, B. and Liskiewicz, M. (2019). Finding minimal d-separators in linear time and applications. In *Proceedings of the 35th Conference on Uncertainty in Artificial Intelligence*.
- Watts, D. J. and Strogatz, S. H. (1998). Collective dynamics of ‘small-world’ networks. *Nature*, 393(6684):440–442.
- Yu, S., Drton, M., and Shojaie, A. (2019). Generalized score matching for non-negative data. *J. Mach. Learn. Res.*, 20:Paper No. 76, 70.
- Zhang, J. (2008). On the completeness of orientation rules for causal discovery in the presence of latent confounders and selection bias. *Artif. Intell.*, 172(16-17):1873–1896.